Model for compound nucleus formation in various heavy-ion systems

V. Yu. Denisov

INFN Laboratori Nazionali di Legnaro, Legnaro, Italy; Institute for Nuclear Research, Kiev, Ukraine; and Faculty of Physics, Taras Shevchenko National University of Kiev, Kiev, Ukraine

(Received 27 September 2023; accepted 8 December 2023; published 8 January 2024)

The statistical model for the calculation of the compound nucleus formation cross section and the probability of compound nucleus formation in heavy-ion collisions is discussed in detail. Light, heavy, and superheavy nucleus-nucleus systems are considered in this model in the framework of one approach. It is shown that the compound nucleus is formed in competition between passing through the compound-nucleus formation barrier and the quasielastic barrier. The compound-nucleus formation barrier is the barrier separating the system of contacting incident nuclei and the spherical or nearly spherical compound nucleus. The quasielastic barrier is the barrier between the contacting and well-separated deformed ions, which are the same as the incident ions. It is shown that the compound nucleus formation cross section is suppressed when the quasielastic barrier is lower than the compound nucleus formation barrier. The critical value of angular momentum, which limits the compound nucleus formation cross-section values for light and medium-mass ion-ion systems at above-barrier collision energies, is discussed in the model. The suppression of the compound nucleus formation cross section even at small partial waves for very heavy ion-ion systems is obtained in the model. The values of the capture and compound nucleus formation cross sections calculated for various light, heavy, and superheavy nucleus-nucleus systems as well as the probability of the compound nucleus formation for superheavy nuclei agree well with the available experimental data.

DOI: 10.1103/PhysRevC.109.014607

I. INTRODUCTION

The collision of light and medium-mass nuclei at energies slightly higher than the nucleus-nucleus interaction barrier for low partial waves leads to the formation of the compound nucleus as a rule. In contrast to this, the formation of compound nuclei in high-energy collisions of light nuclei or in collisions of heavy nuclei at energies slightly higher than the barrier is suppressed [1–24]. The suppression of the compound nucleus formation leads to very low values of the production cross sections of superheavy nuclei [20–51].

Many varied models have been proposed for the description of the compound nucleus formation suppression in heavy ion collisions at energies around the barrier and well above the barrier [1,2,30–63]. In the beginning, the approximation of the critical radius or critical angular momentum [52,53] was proposed for the description of this suppression. Later, the classical friction model was applied for consideration of the compound nucleus formation cross sections [1,2,54,55]. The probability of compound nucleus formation in the collision of very heavy nuclei was also connected to the penetration process through barriers of different nature [31–33,56,57]. The description of the compound nucleus formation is considered in the competition between the direct decay of the stuck-together nuclei into scattered nuclei and the penetration through the barrier related to the sequential nucleon transfer in the direction toward a more asymmetric system of the stuck-together nuclei [34–36,39,40,58,59]. The formation of the compound nucleus is considered as the diffusion process [37,38,41] or as motion with random forces in the complex potential energy landscape, which includes the compound nucleus and separated nuclei [30,42–48]. Often the probability of compound nucleus formation is described by different phenomenological or semiphenomenological expressions with the parameters obtained by fitting the available experimental data [49–51,60–62]. The evaporation residue cross-section is restricted by the fission probability [5,53,63].

A new model for the description of the compound-nucleus formation cross section and probability in collisions of heavy ions is presented. Light, heavy, and superheavy nucleus-nucleus systems are considered in this model in the framework of a single approach. In this model, the compound nucleus is formed in heavy-ion collisions during two consecutive steps.

The first step of the model is related to overcoming the capture barrier, which is formed by the nuclear, Coulomb, and centrifugal interactions of two separated incident nuclei. The capture barrier is associated with colliding nuclei that are in the ground state or have a shape slightly different from that of the ground state due to the fast passing of the capture barrier at high collision energies. The timescale of the barrier passing time at above-barrier heavy-ion collisions is close to 10^{-22} s.

After the barrier passes, the incident nuclei are going to the capture well [64]. The collision energy is quickly transferred into the intrinsic energy of the stuck-together nuclei due to the strong dissipative forces, which take place at the overlap of the densities of interacting nuclei [53–55,65–67]. The relaxation time of the dissipation of radial kinetic energy is smaller than or similar to 10^{-21} s [65–67]. Therefore, the kinetic energy is quickly transferred to the intrinsic energy of both nuclei, and

the temperatures of the nuclear matter in the contacting nuclei are quickly uniform and equal at the end of the first step. So, the system of stuck-together nuclei with zero radial velocity is formed in the capture well. The zero or close to zero radial velocity leads to the dissipation of various memory effects on the future dynamics of the system.

The capture well is limited by a compound nucleus formation barrier $B^{\rm cnf}$ in the case of smaller distances between nuclei. The compound nucleus formation barrier $B^{\rm cnf}$ appears during the smooth shape evolution from the stuck-together incident nuclei to the spherical or near-spherical compound nucleus. The compound nucleus is formed when the system has passed $B^{\rm cnf}$. If the distance between contacting nuclei in the capture well starts to decrease, but the system cannot overcome $B^{\rm cnf}$, then quasifission takes place. The final stage of the quasifission process is scattered nuclei. The compound nucleus can be also formed during the multinucleon transfer from a lighter nucleus to a heavier one [58]. However, the barrier height of this process is higher than $B^{\rm cnf}$, therefore this way of compound nucleus formation is not leading as a rule [39].

The capture well is confined by other barriers in the case of larger distances between nuclei, i.e., on the way from the stuck-together nuclei to the well-separated deformed nuclei. These barriers are formed by the nuclear, Coulomb, and centrifugal interactions of two separated nuclei as well as the contributions of the surface deformation energies of both nuclei. The quasielastic barrier $B^{\rm qe}$ is related to the evolution of the stuck-together nuclei into the same nuclei as incident ones, but deformed, after separation. If the stuck-together nuclei exchange nucleons, the deep-inelastic barrier $B^{\rm di}$ separates the system of the stuck-together and scattered deformed nuclei with new nucleon composition. Note that the quasielastic barrier $B^{\rm qe}$ is, as a rule, the lowest barrier among the barriers on the path of the stuck-together nuclear system to well-separated nuclei.

The second step of the model is linked to the evolution of the system of stuck-together nuclei in the capture well. The nuclear matter of the system in the capture well has a uniform temperature and zero velocity. The stuck-together system in the capture well may be considered as a quasistationary state located in the well between barriers of different nature. Therefore, the further evolution of the system is related to the competition induced by the penetration through the different barriers. The penetration through the different barriers can be considered statistically using the Bohr-Wheeler transition state approximation, which was proposed for the calculation of the width of passing through the fission barrier [68]. As a result, the evolution of the system in the model is linked to the ratio of the widths related to the penetration of the corresponding barriers.

The present model is based on the approximations of the uniform temperature of the nuclear matter and the zero velocity of the stuck-together nuclei at the capture well. The timescale of the shape evolution of the stuck-together nuclei is the main part of the contact time of the heavy-ion fusion-fission reaction [66,69,70]. The contact time is the time interval between the time of touching of incident nuclei and the time of neck breaking between the final nuclei. According to the microscopic calculations, the contact time of the heavy ion reaction is close to ≈ 2–4×10^{-20} s [66,69,70]. Therefore, the process of shape evolution occurring during contact time is much slower than both the capture barrier passing $\approx 10^{-22}$ s and the dissipation time of the kinetic energy $\approx 10^{-21}$ s. The contact time and the time spent by the system in the capture well are of the same order. That is why the system has, as a rule, enough time to settle in the uniform temperature of the nuclear matter and zero velocity in the capture well. As a result, the further evolution of the system of the stuck-together nuclei may be considered statistically using the Bohr-Wheeler transition state approximation.

Note that the uniform temperature of nuclear matter and the zero velocity of the stuck-together nuclei at the capture well cannot be quickly reached for some reactions. For example, a reaction may occur at very high collision energies. Therefore, memory effects may affect the further dynamics of the system in such cases and the present model should be modified.

Due to the very different timescales, the decomposition of the reaction into two steps is natural. The first and fast step is penetration through the capture barrier. The next and relatively slow step is the formation and decay of the stuck-together nuclei. The compound nucleus formation occurs during the decay of the stuck-together nuclei.

For collision of identical or near-identical incident nuclei, the compound nucleus formation barrier $B^{\rm cnf}$ is close to the fission barrier, while for very asymmetric collision systems the height of this barrier is close to the barrier height of the corresponding cluster emission. The cluster emission barrier is related to the strongly asymmetric fission forms and is much higher than the ordinary fission barrier as a rule [71].

The compound nucleus is formed after passing this one-body shape barrier $B^{\rm cnf}$. The quasielastic barrier $B^{\rm qe}$ is, as a rule, the lowest barrier among the barriers on the way from the stuck-together nuclear system to well-separated nuclei. Therefore, the competition when the nuclear system passes through the barriers $B^{\rm cnf}$ and $B^{\rm qe}$ determines the probability of the compound nucleus formation. As a result, the compound nucleus formation cross section is connected to the probability of its formation as well as the penetration through the capture barrier between the incident nuclei.

The next section of the paper is related to the description of the model. The discussion of the model application to various heavy ion systems is presented in Sec. III. The conclusions are given in Sec. IV.

II. THE MODEL

The total interaction potential of two spherical nuclei at the distance between their mass centers r larger the contact distance consists of the Coulomb $V^0_{\rm C}(r) = Z_1 Z_2 e^2/r$, nuclear $V^0_{\rm N}(r)$, and centrifugal potential energies, i.e.,

$$V^{\rm t}_\ell(r) = V^0_{\rm C}(r) + V^0_{\rm N}(r) + \hbar^2 \ell(\ell+1)/(2\mu r^2). \qquad (1)$$

Here Z_i is the number of protons in the incident nucleus i, $i = 1, 2$, e is the charge of the proton, and μ is the reduced mass.

The potential $V_\ell^{\rm t}(r)$ has, as a rule, the capture barrier and the capture well at low values of the angular momentum ℓ [64]. The distance between the closest points of the surfaces of colliding nuclei belongs to the range 1–2.5 fm at the capture barrier point. The stuck-together nuclei are formed after penetration through this barrier. Therefore, the formation cross section of the stuck-together nuclei or the capture cross section is

$$\sigma^{\rm c}(E) = \sum_{\ell=0}^{\infty} \sigma_\ell^{\rm c}(E) = \frac{\pi\hbar^2}{2\mu E} \sum_{\ell=0}^{\infty} (2\ell+1) T_\ell(E). \tag{2}$$

Here $\sigma_\ell^{\rm c}(E)$ is the partial wave cross section and E is the energy of collision in the center-of-mass system. The transmission coefficient through the capture barrier $T_\ell(E)$ can be calculated using the Ahmed formula [72]

$$T_\ell(E) = \frac{1-\exp\left(-4\pi\alpha_\ell\right)}{1+\exp\left[2\pi\left(\beta_\ell-\alpha_\ell\right)\right]}, \tag{3}$$

where $\alpha_\ell = \frac{2(B_\ell^{\rm sph}E)^{1/2}}{\hbar\omega_\ell}$ and $\beta_\ell = \frac{2B_\ell^{\rm sph}}{\hbar\omega_\ell}$. Here $B_\ell^{\rm sph} = V_\ell^{\rm t}(r_b)$ is the capture barrier height, r_b is the radius of the barrier, and $\hbar\omega_\ell = (-\frac{\hbar^2}{\mu}\frac{d^2V_\ell^{\rm t}(r)}{dr^2})^{1/2}|_{r=r_b}$ is the barrier curvature. Ahmed obtained the exact expression for the transmission coefficient through the Morse potential barrier [73]. The shape of the realistic total nucleus-nucleus potential is closer to the shape of the Morse potential than the parabolic one; see for details Ref. [74] and papers cited therein. Therefore, Ahmed's expression for the transmission coefficient is more suitable than the corresponding expression for the parabolic barrier [75,76]. The difference between the Ahmed and parabolic transmission coefficients is important for sub-barrier energies [74].

The stuck-together nuclei are populated states at the capture well of the total potential as a rule [64]. The kinetic energy of relative motion is, as a rule, completely dissipated into inner degrees of freedom due to the strong dissipation caused by the overlap of some parts of approaching nuclei during the collision [53–55,65–67]. The uniform temperature of nuclear matter is quickly set in the system of the stuck-together nuclei. Therefore, all subsequent evolution stages of the stuck-together nuclei can be considered using the Bohr-Wheeler transition state approximation.

The compound nucleus formation cross section is connected to both the penetration through the capture barrier and the probability of the compound nucleus formation. Therefore, the cross section of the compound nucleus formation is

$$\sigma^{\rm cn}(E) = \sum_{\ell=0}^{\infty} \sigma_\ell^{\rm cn}(E) = \frac{\pi\hbar^2}{2\mu E} \sum_{\ell=0}^{\infty} (2\ell+1) T_\ell(E) P_\ell(E), \tag{4}$$

where

$$P_\ell(E) = \frac{\Gamma_\ell^{\rm cn}(E)}{\Gamma_\ell^{\rm s}(E)} = \frac{1}{1+G_\ell(E)} \tag{5}$$

is the compound nucleus formation probability in the partial wave ℓ. Here $\Gamma_\ell^{\rm cn}(E)$ is the decay width of the stuck-together nuclei to the compound nucleus states,

$$\Gamma_\ell^{\rm s}(E) = \Gamma_\ell^{\rm cn}(E) + \Gamma_\ell^{\rm d}(E) \tag{6}$$

is the total decay width of the state of the stuck-together nuclei, and

$$G_\ell(E) = \frac{\Gamma_\ell^{\rm d}(E)}{\Gamma_\ell^{\rm cn}(E)}. \tag{7}$$

$\Gamma_\ell^{\rm d}(E)$ is the decay width of the stuck-together nuclei into all channels leading to the two separated nuclei.

The width $\Gamma_\ell^{\rm d}(E)$ includes the contributions of the elastic $\Gamma_\ell^{\rm e}(E)$, quasielastic $\Gamma_\ell^{\rm qe}(E)$, and single- and many-particle transfers $\Gamma_\ell^{\rm t}(E)$, and of the deep-inelastic $\Gamma_\ell^{\rm di}(E)$ and quasi-fission $\Gamma_\ell^{\rm qf}(E)$ decays of the stuck-together nuclei [39]. As a result, $\Gamma_\ell^{\rm d}(E) = \Gamma_\ell^{\rm e}(E) + \Gamma_\ell^{\rm qe}(E) + \Gamma_\ell^{\rm t}(E) + \Gamma_\ell^{\rm di}(E) + \Gamma_\ell^{\rm qf}(E)$. The quasielastic barrier $B^{\rm qe}$ has the lowest barrier height among these processes [39]. Therefore, the width of the quasielastic decay of the stuck-together nuclei is the leading contribution to $\Gamma_\ell^{\rm d}(E)$, i.e., $\Gamma_\ell^{\rm d}(E) \approx \Gamma_\ell^{\rm qe}(E)$.

Besides this, the experimental mass distributions of binary products formed in the reactions leading to the heavy and superheavy nuclei at energies around and higher the Coulomb barrier have the strongest yields for the quasielastic events, while the yields of other processes are much smaller [4,7,14,15,17,22–24]. The quasielastic contribution to the cross section is the leading one for high-energy collisions of various heavy ions [77,78]. These experimental observations support the approximation $\Gamma_\ell^{\rm d}(E) \approx \Gamma_\ell^{\rm qe}(E)$.

The compound nucleus can be formed by passing through the compound nucleus formation barrier $B^{\rm cnf}$. As pointed out in the Introduction, multinucleon transfer can also lead to the compound nucleus formation [58]. However, the one-body barrier $B^{\rm cnf}$ is lower than the two-body barrier related to the compound nucleus formation during multinucleon transfer [39]. Therefore, the compound nucleus is mainly formed when passing through the barrier $B^{\rm cnf}$, and the contribution of the compound nucleus formation through multinucleon transfer to $\Gamma_\ell^{\rm cn}(E)$ may be neglected.

So, the widths describing the passage through the barriers $B^{\rm cnf}$ and $B^{\rm qe}$, i.e., $\Gamma_\ell^{\rm cn}(E)$ and $\Gamma_\ell^{\rm qe}(E)$, are the most important for calculations of $G_\ell(E)$ and $P_\ell(E)$. Consequently, using the discussed approximations for the widths $\Gamma_\ell^{\rm d}(E)$ and $\Gamma_\ell^{\rm cn}(E)$, one can write

$$G_\ell(E) \approx \frac{\Gamma_\ell^{\rm qe}(E)}{\Gamma_\ell^{\rm cn}(E)}. \tag{8}$$

The total probability of compound nucleus formation in heavy-ion collision is

$$P(E) = \frac{\sigma^{\rm cn}(E)}{\sigma^{\rm c}(E)} = \frac{\sum_{\ell=0}^{\infty}(2\ell+1)T_\ell(E)P_\ell(E)}{\sum_{\ell=0}^{\infty}(2\ell+1)T_\ell(E)}. \tag{9}$$

This probability is sometimes studied experimentally; see Refs. [4,8,15,20,24] and Figs. 4 and 5.

As follows from Eqs. (4), (5), and (8), to calculate the cross section for the formation of a compound nucleus, it

is necessary to know the widths $\Gamma_\ell^{\rm cn}(E)$ and $\Gamma_\ell^{\rm qe}(E)$. These widths are discussed in the next subsections in detail.

A. The width $\Gamma_\ell^{\rm cn}(E)$

The width $\Gamma_\ell^{\rm cn}(E)$ can be linked to the compound nucleus formation barrier $B^{\rm cnf}$, which exists during the smooth shape evolution from the stuck-together nuclei to the spherical or nearly spherical compound nucleus. This barrier $B^{\rm cnf}$ is related to the one-body shape evolution as the ordinary fission barrier. The minimal value of $B^{\rm cnf}$ may be estimated as the height of the fission barrier because the probability of fission is related to the trajectory of minimal action [79], which connects the compound nucleus and the two separated nuclei. Note that during heavy-ion fusion and fission, the collective coordinates describing these processes are changed in opposite directions. Therefore, the width $\Gamma_\ell^{\rm cn}(E)$ can be found similarly to the fission width, applying the Bohr-Wheeler approximation of the transition state [68].

The width for passing the fission barrier was introduced by Bohr and Wheeler in 1939 [68]. Note that the Bohr-Wheeler fission width is obtained for the fission barrier height independently of the thermal energy of the fissioning system.

As was shown by Strutinsky in 1966, the fission barrier height consists of the liquid-drop and shell-correction contributions [79–82]. It was found in 1972 that the shell correction energy decreases strongly with an increase of the inner energy ε of the system [83]. Due to this, the height of the fission barrier depends very strongly on the inner energy ε of the system [83–91].

A simple expression for the fission width of excited nuclei with the fission barrier dependent on excitation energy is derived in Ref. [90]. At the zero-excitation energy the fission width derived in Ref. [90] coincides with the Bohr-Wheeler width. The expression obtained in Ref. [90] leads to a good description of the experimental values of the ratio $\Gamma_{\rm f}(E)/\Gamma_{\rm n}(E)$ and the fission barrier heights in various nuclei [89,91]. Here $\Gamma_{\rm n}(E)$ is the neutron evaporation width.

Taking into account that the fusion and fission are somehow mutually inverse processes and modifying the expression for the fission width derived in Ref. [90], the width for passing the compound nucleus formation barrier in heavy-ion collisions can be written as

$$\Gamma_\ell^{\rm cn}(E) = \frac{2}{2\pi\rho_{\rm sn}(E)}\int_0^{\varepsilon_{\rm m}} d\varepsilon \frac{\rho_A(\varepsilon)}{N_{\rm tot}} N_{\rm s}(\varepsilon). \tag{10}$$

Here $\rho_{\rm sn}(E)$ is the level density of the stuck-together nuclei (the level density of the initial state), $\rho_A(\varepsilon)$ is the level density of the compound nucleus with A nucleons formed in the heavy-ion collision, the ratio $\rho_A(\varepsilon)/N_{\rm tot}$ is the probability of finding the nuclear system passing through the barrier with the intrinsic (thermal) excitation energy ε in the above-barrier transition states,

$$N_{\rm tot} = \int_0^{\varepsilon_{\rm m}} d\varepsilon \rho_A(\varepsilon) \tag{11}$$

is the total number of states available for barrier passing in the case of the energy-dependent barrier of compound nucleus formation $B_{\rm cnf}(\varepsilon)$,

$$N_{\rm s}(\varepsilon) = \int_0^{E+Q-B_\ell^{\rm cnf}(\varepsilon)-\varepsilon} dK\, \rho_A(E+Q-B_{\rm cnf}(\varepsilon)-K) = \int_\varepsilon^{E+Q-B_\ell^{\rm cnf}(\varepsilon)} de \rho_A(e) \tag{12}$$

is the number of states available for the nuclear system passing through the barrier at the thermal excitation energy ε, and Q is the fusion reaction Q value. Note that $B_\ell^{\rm cnf}(\varepsilon)$ and $E+Q$ are, respectively, the barrier height and the excitation energy of the compound nucleus evaluated relative the ground state of the compound nucleus formed in the fusion reaction. $\varepsilon_{\rm m}$ is the maximum value of the thermal excitation energy of the compound nucleus at the saddle point, which is determined as the solution of the equation

$$\varepsilon_{\rm m} + B_\ell^{\rm cnf}(\varepsilon_{\rm m}) = E + Q. \tag{13}$$

This equation is related to the energy conservation law; i.e., the sum of thermal $\varepsilon_{\rm m}$ and potential $B_{\rm cnf}(\varepsilon_{\rm m})$ energies at the saddle point equals the total excitation energy $E+Q$.

The back-shifted Fermi gas model [92,93] is used for a description of the level density $\rho_A(\varepsilon)$ of the nucleus with A nucleons. The level density in this model is given by

$$\rho_A(\varepsilon) = \frac{\pi^{1/2}\exp\left[2\sqrt{a_A(\varepsilon-\Delta)(\varepsilon-\Delta)}\right]}{12[a_A(\varepsilon-\Delta)]^{1/4}(\varepsilon-\Delta)^{5/4}}, \tag{14}$$

where

$$a_A(\varepsilon) = a_A^0\left\{1+\frac{E_{\rm shell}^{\rm emp}}{\varepsilon}[1-\exp(-\gamma\varepsilon)]\right\} \tag{15}$$

is the level density parameter [93,94]. Here

$$a_A^0 = 0.0722396A + 0.195267A^{2/3}\ {\rm MeV}^{-1} \tag{16}$$

is the asymptotic level density parameter obtained at high excitation energies, when all shell effects are damped [93,94], $E_{\rm shell}^{\rm emp}$ is the empirical shell correction value [93,95], $\gamma = 0.410289/A^{1/3}\ {\rm MeV}^{-1}$ is the damping parameter [93,94], and A is the number of nucleons in the nucleus. According to the prescription of Ref. [93], the value of empirical shell correction $E_{\rm shell}^{\rm emp}$ is calculated as the difference between the experimental value of nuclear mass and the liquid-drop component of the mass formula [93,95]. The back-shift energy is described by the expression $\Delta = 12n/A^{1/2} + 0.173015$ MeV [93], where $n = -1$, 0, and 1 for odd-odd, odd-A, and even-even nuclei, respectively.

According to the Strutinsky shell correction prescription [79–86,89–91] the barrier height of compound nucleus formation is written as

$$B_\ell^{\rm cnf}(\varepsilon) = B_\ell^{\rm ld}(\varepsilon) + B_\ell^{\rm sh}(\varepsilon) + \frac{\hbar^2\ell(\ell+1)}{2J^{\rm cnf}}. \tag{17}$$

Here

$$B_\ell^{\rm ld}(\varepsilon) = E_\ell^{\rm saddle\ ld}(\varepsilon) - E_\ell^{\rm gs\ ld}(\varepsilon) \tag{18}$$

is the liquid-drop contribution to the barrier and

$$B_\ell^{\rm sh}(\varepsilon) = E_\ell^{\rm saddle\ sh}(\varepsilon) - E_\ell^{\rm gs\ sh}(\varepsilon) \tag{19}$$

is the shell contribution to the compound nucleus formation barrier related to the nonuniform distribution of the single-particle energies around the Fermi level. Here $E_\ell^{\text{saddle ld/sh}}$ and $E_\ell^{\text{gs ld/sh}}$ are the liquid-drop/shell-correction energies of the nucleus at the saddle and ground-state points, respectively. The last term in Eq. (17) is the rotational contribution. $J^{\text{cnf}} = \frac{2}{5}MR_0^2A(1+\sqrt{\frac{5}{16\pi}}\beta_{\text{cnf}}+\frac{135}{84\pi}\beta_{\text{cnf}}^2)$ is the moment of inertia of the nucleus at the compound nucleus formation barrier, where $R_0 = r_0A^{1/3}$ is the radius of a spherical compound nucleus, β_{cnf} is the quadrupole deformation of the nucleus at the barrier, and M is the nucleon mass. The axial symmetry axis of the nucleus is perpendicular to the rotation axis. The contribution of octupole deformation to the moment of inertia may be neglected because the octupole deformation value is smaller than the quadrupole one. The contributions of higher multipole deformations to the moment of inertia are small as a rule due to small values of higher multipole deformations. The pairing force contribution to the compound nucleus formation barrier is ignored here because this contribution is strongly attenuated or zero at high excitation energies of the nucleus formed in heavy-ion collisions. Recall that the pairing force is reduced with the temperature and disappears at the critical temperature $T \approx 0.5$ MeV [90]. The temperature of the compound nucleus system formed in heavy-ion fusion reactions is sufficiently high as a rule.

The temperature dependence of the constants of the liquid-drop model is negligible at $T \lesssim 2$ MeV and small for higher temperatures [96,97]. Due to this, the liquid-drop contribution to the compound nucleus formation barrier height $B_\ell^{\text{ld}}(\varepsilon)$ depends weakly on the thermal excitation energy ε [89,90,96,97]. Therefore, the temperature dependence of the liquid-drop contribution to the compound nucleus formation barrier is ignored.

The exponential damping of the single-particle shell-correction contribution into the fission barrier with an increase of ε is widely discussed; see Refs. [31,39,86–88,90] and papers cited therein. The exponential damping of the fission barriers of various superheavy nuclei with an increase ε has been confirmed in the framework of the finite-temperature self-consistent Hartree-Fock+BCS approach with the Skyrme force [87,88]. The results of the shell correction calculations [86] show similar behavior. Therefore, this approximation can be also applied to the compound nucleus formation barrier because the fission and compound nucleus formation barriers are related to the variation of the nuclear system energy with deformation. Then, the compound nucleus formation barrier can be approximated as

$$B_\ell^{\text{cnf}}(\varepsilon) \approx B^{\text{ld}} + B^{\text{sh}}\exp(-\gamma_D\varepsilon) + \frac{\hbar^2\ell(\ell+1)}{2J^{\text{cnf}}}. \quad (20)$$

Here $B^{\text{ld}} = B_{\ell=0}^{\text{ld}}(0)$ and $B^{\text{sh}} = B_{\ell=0}^{\text{sh}}(0)$ are, respectively, the liquid-drop and shell correction contributions to the compound nucleus formation barrier at $\varepsilon = 0$ and $\ell = 0$, and γ_D is the damping coefficient. The dependencies of B^{ld}, B^{sh}, and J^{cnf} on ℓ are neglected for the sake of simplicity.

The values of $B^{\text{sh}} \approx -E_{\ell=0}^{\text{gs sh}}(0) = -E^{\text{gs sh}}$ because $|E_\ell^{\text{gs sh}}(0)| \gg |E_\ell^{\text{saddle sh}}(0)|$ as a rule; see Refs. [31,91] and papers cited therein. As a result, Eq. (20) can be written as

$$B_\ell^{\text{cnf}}(\varepsilon) \approx B^{\text{ld}} - E^{\text{gs sh}}\exp(-\gamma_D\varepsilon) + \frac{\hbar^2\ell(\ell+1)}{2J^{\text{cnf}}}. \quad (21)$$

Note that the values of $E^{\text{gs sh}}$ obtained in the framework of the macroscopic-microscopic model are tabulated in Refs. [98,99] for many nuclei. The values of the ground-state shell correction energy given in Ref. [98] are used in the calculations of the fission barrier. Besides this, the values of $E^{\text{gs sh}}$ can be also found empirically; see for details the next subsection.

In the case of collision of identical or near identical nuclei the values of B^{ld} can be found using the code BARFIT [100] with the original values of parameters because the compound nucleus formation barrier is close to the fission barrier. The values of the fission barrier calculated in the macroscopic-microscopic finite-range liquid-drop model [101] can be used for fixing the barrier values too. So, there are various possibilities to define the liquid-drop and shell-correction contributions of the compound nucleus formation barrier for a nearly symmetric collision system.

For collisions involving very different nuclei the values of B^{ld} should be larger than the one calculated for the symmetric fission using the code BARFIT. The compound nucleus formation barrier for symmetric [32,33] and asymmetric [31,39] heavy ion systems leading to the superheavy nuclei are discussed in the framework of simplified calculations. The approximation used to describe the cluster decay [71] can also be applied to evaluate the compound nucleus formation barrier for asymmetric systems. Note that the asymmetric fission shapes are important for the heavy and superheavy nuclei [102,103]. The B^{ld} value may also be used as the model's fitting parameter.

It is well known that the shell-correction energy disappears in various nuclei at a compound-nucleus temperature of $T_D \approx 2$ MeV [83–85]. Due to this, the compound nucleus formation barrier height is only determined by the liquid-drop contribution at $T \gtrsim 2$ MeV. The compound-nucleus excitation energy ε at high T is $\varepsilon = a_A^0T^2$, where a_A^0 is defined in Eq. (16). Applying $E^{\text{sh}}(\varepsilon_D) = E^{\text{sh}}(0)\ \exp(-\gamma_D\varepsilon_D)$, where $\varepsilon_D = a_A^0T_D^2$, it is easy find $\gamma_D = \ln[E^{\text{sh}}(0)/E^{\text{sh}}(\varepsilon_D)]/a_A^0T_D^2$. Substituting $E^{\text{sh}}(0)/E^{\text{sh}}(\varepsilon_D) \approx 100$ and using (16) one obtains a simple formula for calculation of the damping coefficient, $\gamma_D \approx 1.15/(0.0722396A + 0.195267A^{2/3})$ MeV^{-1}. The values of γ_D calculated by this formula for the range $180 \lesssim A \lesssim 300$ are close to values used in other works [31,39,49,50,87,91].

It may seem that the parameters γ_D in Eqs. (20) and (21) and γ in Eq. (15) should be the same because these parameters relate to the damping of the shell structure with rising excitation energy of the compound nucleus. However, this is not correct. The parameter γ is obtained by fitting the experimental data for the energy level densities in different nuclei for various excitation energies using Eq. (14) with the phenomenological dependence of the level density parameter described by Eq. (15) [93,94]. The experimental data for the energy level densities include the single-particle levels, multiparticle-multihole levels, and other levels of various natures. The value of γ_D is only related to the structure of the single-particle levels around the Fermi energy, which are

taken into account in the shell-correction method [79–88]. The value of γ smoothly decreases with the number of nucleons in nuclei, because $\gamma \propto A^{-1/3}$. In contrast to this, the parameter γ_D is obtained using the disappearance of the shell-correction energy at $T_D \approx 2$ MeV and $\gamma_D \propto A^{-1}$.

B. The width $\Gamma_\ell^{\rm qe}(E)$

The energy dependence of the quasielastic barrier can be neglected. Therefore, the Bohr-Wheeler approximation of the transition state [68] can be used for the calculation of the width $\Gamma_\ell^{\rm qe}(E)$. The width $\Gamma_\ell^{\rm qe}(E)$ is related to the combination of level densities in two nuclei, so

$$\Gamma_\ell^{\rm qe}(E) = \frac{1}{2\pi\,\rho_{\rm sn}(E)} \int_0^{E-B_\ell^{\rm qe}} d\varepsilon \int_0^{\varepsilon} d\epsilon\ \rho_{A_1}(\epsilon) \times \rho_{A_2}(\varepsilon-\epsilon). \tag{22}$$

Here $B_\ell^{\rm qe}$ is the value of the quasielastic barrier calculated relative to the interaction potential energy of two nuclei at infinite distance between them. The energy level densities $\rho_{\rm sn}(E)$ and $\rho_{A_i}(\epsilon)$ are determined in Eqs. (10) and (14), respectively. A_i is the number of nucleons in incident nucleus i, $i = 1, 2$, and $A = A_1 + A_2$ is the number of nucleons in the compound nucleus.

The value of barrier height $B_\ell^{\rm qe}$ is calculated as the lowest barrier of the total potential energy of two nuclei, which separates the stuck-together and well-separated deformed nuclei. The total potential energy of deformed nuclei is

$$\begin{aligned} V_\ell^{\rm t}(r,\{\beta_1\},\{\beta_2\}) =& V_{\rm C}(r,\{\beta_1\},\{\beta_2\}) \\ &+ V_{\rm N}(r,\{\beta_1\},\{\beta_2\}) + V_\ell(r,\{\beta_1\},\{\beta_2\}) \\ &+ E^1_{\rm def}(\{\beta_1\}) + E^2_{\rm def}(\{\beta_2\}), \end{aligned} \tag{23}$$

where $\{\beta_i\} = \beta_{i2}, \beta_{i3}$ are the surface deformation parameters of nucleus i with the surface radius $R_i(\theta) = R_{0i}[1 + \sum_{L=2,3} \beta_{iL} Y_{L0}(\theta)]$, $i = 1, 2$, R_{0i} is the radius of the spherical nucleus, and $Y_{L0}(\theta)$ is the spherical harmonic function [104]. $V_{\rm C}(r,\{\beta_1\},\{\beta_2\})$, $V_{\rm N}(r,\{\beta_1\},\{\beta_2\})$, and $V_\ell(r,\{\beta_1\},\{\beta_2\})$ are the Coulomb, nuclear, and centrifugal potentials of deformed nuclei, respectively. $E_{\rm def}(\{\beta_i\})$ is the deformation energy of nucleus i.

The lowest barrier is related to axial-symmetric nuclei both elongated along the axis connecting their mass centers [64,105]. The Coulomb interaction of two axial-symmetric deformed nuclei at such mutual orientation is

$$\begin{aligned} &V_{\rm C}(r,\{\beta_1\},\{\beta_2\}) \\ &= V_{\rm C}^0(r)\big[1 + f_1(r,R_{01})\beta_{12} \\ &\quad + f_1(r,R_{02})\beta_{22} + f_2(r,R_{01})\beta_{12}^2 + f_2(r,R_{02})\beta_{22}^2 \\ &\quad + f_3(r,R_{01},R_{02})\beta_{12}\beta_{22} + f_4(r,R_{01})\beta_{13} + f_4(r,R_{02})\beta_{23} \\ &\quad + f_5(r,R_{01})\beta_{13}^2 + f_5(r,R_{02})\beta_{23}^2 + f_6(r,R_{01},R_{02})\beta_{13}\beta_{23} \\ &\quad + f_7(r,R_{01})\beta_{12}\beta_{13} + f_7(r,R_{02})\beta_{22}\beta_{23} \\ &\quad + f_8(r,R_{01},R_{02})\beta_{12}\beta_{23} + f_8(r,R_{02},R_{01})\beta_{22}\beta_{13}\big], \end{aligned} \tag{24}$$

where $V_{\rm C}^0(r)$ is the Coulomb interactions of spherical nuclei [see Eq. (1)] and r is the distance between their mass centers [106]. Here

$$f_1(r,R_{0i}) = \frac{3R_{0i}^2}{2\sqrt{5\pi}\,r^2}, \tag{25}$$

$$f_2(r,R_{0i}) = \frac{3R_{0i}^2}{7\pi r^2} + \frac{9R_{0i}^4}{14\pi r^4}, \tag{26}$$

$$f_3(r,R_{01},R_{02}) = \frac{27R_{01}^2R_{02}^2}{10\pi r^4}, \tag{27}$$

$$f_4(r,R_{0i}) = \frac{3R_{0i}^3}{2\sqrt{7\pi}\,r^3}, \tag{28}$$

$$f_5(r,R_{0i}) = \frac{2R_{0i}^2}{5\pi r^2} + \frac{9R_{0i}^4}{22\pi r^4} + \frac{100R_{0i}^6}{143\pi r^6}, \tag{29}$$

$$f_6(r,R_{01},R_{02}) = \frac{45R_{01}^3R_{02}^3}{7\pi r^6}, \tag{30}$$

$$f_7(r,R_{0i}) = \frac{\sqrt{5}R_{0i}^3}{\sqrt{7}\pi r^3} + \frac{5\sqrt{35}R_{0i}^5}{22\pi r^5}, \tag{31}$$

$$f_8(r,R_{01},R_{02}) = \frac{9\sqrt{5}R_{01}^2R_{02}^3}{2\sqrt{7}\pi r^5}. \tag{32}$$

This expression for $V_{\rm C}(r,\{\beta_1\},\{\beta_2\})$ takes into account all linear and quadratic terms of both the quadrupole and octupole deformation parameters. The octupole deformation parameters are chosen in such a way that the shapes of two identical nuclei are mirror symmetric with respect to the plane passing through half of the distance between the surfaces of the nuclei and perpendicular to the axial-symmetry axis of the system. The volume correction, which appears in the second order of the deformation parameter and is important for heavy systems, is taken into account in this expression. The volume correction is connected to the conservation of the particle number in the nucleus. Note that the position of the mass center of a nucleus with nonzero quadrupole and octupole deformations is slightly shifted from the position of the mass center of a spherical nucleus. This shift is proportional to $\beta_{i2}\beta_{i3}$ [107–109]. The additional dipole deformations, which are proportional to $\beta_{i1} \propto -\beta_{i2}\beta_{i3}$, are introduced for the compensation of this shift of the mass center position; see for details Refs. [108,109]. As a result, deformed and spherical nuclei have the same positions as the mass centers. Therefore, the distances between the mass centers of the deformed and spherical nuclei are the same in the present approach.

According to the proximity theorem [110,111], the nuclear part of nucleus-nucleus interaction is determined by the closest distance between surfaces of these nuclei, $d(r)$. A function dependent on $d(r)$ parameterizes the dependence of the nucleus-nucleus interaction potential on $d(r)$ [111]. This function is different for various parametrizations of the proximity-type potentials [111–114]. According to the proximity theorem, the nuclear interaction of deformed nuclei at the closest distance between surfaces, $d(r,\beta_1,\beta_2)$, links to the nuclear interaction of these spherical nuclei located at the same closest distance between surfaces of the spherical nuclei, $d_{\rm sph}(r_{\rm sph})$, i.e., when

$$d(r,\beta_1,\beta_2) = d_{\rm sph}(r_{\rm sph}). \tag{33}$$

Here

$$d(r,\{\beta_1\},\{\beta_2\}) = r - R_1(0) - R_2(0), \quad (34)$$

$$d_{\rm sph}(r_{\rm sph}) = r_{\rm sph} - R_{0\rm t}, \quad (35)$$

and $R_{0\rm t} = R_{01} + R_{02}$. Note that the distances between mass centers of the spherical $r_{\rm sph}$ and deformed r nuclei are different.

The nuclear part of the interaction potential between deformed nuclei in the proximity approach [39,106,115,116] is

$$V_{\rm N}(r,\{\beta_1\},\{\beta_2\}) = S(\{\beta_1\},\{\beta_2\}) \times V_{\rm N}^0(d(r,\{\beta_1\},\{\beta_2\}) + R_{0\rm t}). \quad (36)$$

Here

$$S(\{\beta_1\},\{\beta_2\}) = \frac{\frac{R_1(\pi/2)^2R_2(\pi/2)^2}{R_1(\pi/2)^2R_2(0)+R_2(\pi/2)^2R_1(0)}}{\frac{R_{01}R_{02}}{R_{0\rm t}}} \quad (37)$$

is the factor related to the modification of the strength of nuclear interaction induced by the surface deformations of the interacting nuclei, which is derived in Ref. [115]. Recall that the octupole deformation parameters are chosen in such a way that the shape of two identical nuclei is mirror symmetric with respect to the plane passing through half of the distance between the surfaces of the nuclei and perpendicular to the axial-symmetry axis of the system.

The potential $V_{\rm N}^0$ determines the nuclear part of the interaction between spherical nuclei, which consists of the macroscopic and the shell-correction contributions to the interacting energy of nuclei [39,106,112,117–119],

$$V_{\rm N}^0(r) = V_{\rm macro}(r) + V_{\rm sh}(r). \quad (38)$$

Here r is the distance between the mass centers of spherical nuclei.

The macroscopic part $V_{\rm macro}(r)$ of the nuclear interaction of nuclei is related to the macroscopic density distribution and the nucleon-nucleon interactions of colliding nuclei. At $r > R_{0\rm t}$, it has the Woods-Saxon form [39,106,112]

$$V_{\rm macro}(r) = \frac{v_1C + v_2C^{1/2}}{1+\exp[(r-R_{0\rm t})/(d_1+d_2/C)]}. \quad (39)$$

Here $v_1 = -27.190$ MeV fm^{-1}, $v_2 = -0.93009$ MeV fm$^{-1/2}$, $d_1 = 0.78122$ fm, $d_2 = -0.20535$ fm^2, $C = R_{01}R_{02}/R_{0\rm t}$ is in fm, $R_{0i} = 1.2536A_i^{1/3} - 0.80012A_i^{-1/3} - 0.0021444/A_i$ is the radius of ith nucleus in fm, and A_i is the nucleon number in the nucleus i.

The shell-correction contribution $V_{\rm sh}(r)$ to the nucleus-nucleus potential is related to the shell structure of nuclei, which is disturbed by the nucleon-nucleon interactions of colliding nuclei. When the nuclei approach each other, the energies of the single-particle nucleon levels of each nucleus are shifted and split due to the interaction of nucleons belonging to different nuclei [118,119]. Therefore, the energy level spectra near the Fermi energy become more uniform. This leads to the reduction of the amplitude of the shell correction energy at small distances between interacting nuclei. Due to this, the shell-correction contribution to the nuclear part of the interaction between nuclei is introduced in Refs. [106,112,117]. The representation of the nucleus-nucleus potential energy in Eq. (38) is similar to the Strutinsky shell-correction prescription [79–82,118,119], which is widely used for the calculation of the nuclear binding energies, the deformation energies, the fission barriers, the cluster emission barrier, and other quantities. The shell-correction part of the nucleus-nucleus potential at $r > R_{\rm t}$ is given as [39,106,112]

$$V_{\rm sh}(r) = \left[E_1^{\rm gs\ sh} + E_2^{\rm gs\ sh}\right]\left[\frac{1}{1+\exp\left(\frac{R_{\rm sh}-R}{d_{\rm sh}}\right)} - 1\right], \quad (40)$$

where $R_{\rm sh} = R_{0\rm t} - 0.26$ fm, $d_{\rm sh} = 0.233$ fm, and

$$E_i^{\rm gs\ sh} = B_i^{\rm m} - B_i^{\rm exp}(A,Z) \quad (41)$$

is the phenomenological shell correction for nucleus i. Here

$$B_i^{\rm m} = 15.86864A_i - 21.18164A_i^{2/3} + 6.49923A_i^{1/3} - \left[\frac{N_i-Z_i}{A_i}\right]^2\left[26.37269A_i - 23.80118A_i^{2/3} - 8.62322A_i^{1/3}\right] - \frac{Z_i^2}{A_i^{1/3}}\left[0.78068 - 0.63678A_i^{-1/3}\right] - P_p - P_n \quad (42)$$

is the macroscopical value of the binding energy in MeV established in the phenomenological approach, and $B_{\rm exp}(A,Z)$ is the binding energy of the nucleus in MeV obtained using the evaluated atomic masses [120]. $P_{p(n)}$ are the proton (neutron) pairing terms, which are equal to $P_{p(n)} = 5.62922\,(4.99342)\,A_i^{-1/3}$ in the case of odd Z (N) and $P_{p(n)} = 0$ in the case of even Z_i (N_i), and N_i is the neutron number in the nucleus i. Equations (41) and (42) may be used for calculation of $E^{\rm gs\ sh}$ in Eq. (21) too.

The values of $V_{\rm sh}(r)$ are close to zero at large distances between nuclei. The values of $V_{\rm sh}(r) \approx [E_1^{\rm gs\ sh} + E_2^{\rm gs\ sh}]/2$ at small distances between nuclei. The shell-correction contribution to the total nuclear interaction of nuclei takes into account the individual peculiarities of the nuclei involved in the collision. It is related to the deviation of the total nuclear interaction from the global macroscopic interaction.

The centrifugal potential energy of two deformed nuclei is presented in the form traditional for heavy ions,

$$V_\ell(r,\{\beta_{1L}\},\{\beta_{2L}\}) = \frac{\hbar^2\ell(\ell+1)}{2J^{\rm qe}}. \quad (43)$$

Here $J^{\rm qe} = \mu r^2$ is the moment of inertia of the quasielastic system and μ is the reduced mass; see also Eq. (1).

The deformation energy of the nucleus induced by the surface multipole deformations is

$$E_{\rm def}^i(\{\beta_{iL}\}) = \sum_{L=2}^{3}\left[C_{LA_iZ_i}^{\rm ld} + C_{LA_iZ_i}^{\rm sh}\right]\frac{\beta_{iL}^2}{2}. \quad (44)$$

Here

$$C_{LA_iZ_i}^{\rm ld} = \frac{(L-1)(L+2)b_{\rm surf}A_i^{2/3}}{4\pi} - \frac{3(L-1)e^2Z_i^2}{2\pi(2L+1)R_{0i}} \quad (45)$$

is the surface stiffness coefficient obtained in the liquid-drop approximation [107,121], and $b_{\rm surf}$ is the surface coefficient

of the mass formula [98]. $C_{\rm sc}$ is the shell-correction contribution to the stiffness coefficient. It is possible to approximate $C^{\rm sc} \approx -0.05\,\delta E\,C^{\rm ld}$ [39,122], where δE is the phenomenological shell-correction value in MeV; see Eq. (41). Note that experimental values of the surface stiffness coefficient for different nuclei are distributed around the value $C^{\rm ld}$ [107,121]. The approximation for the surface stiffness coefficient used in Eq. (45) is crude, but it is taken into account by the shell effect. This approximation corresponds to the experimental tendency of the values of the surface stiffness coefficient and simplifies further calculations significantly.

So, the integrals in the widths $\Gamma_\ell^{\rm cn}(E)$ and $\Gamma_\ell^{\rm qe}(E)$ [see Eqs. (10) and (22)] have been defined. Note that both widths $\Gamma_\ell^{\rm d}(E)$ and $\Gamma_\ell^{\rm qe}(E)$ are inversely proportional to the level density of the stuck-together nuclei, $\rho_{\rm sn}(E)$. Therefore, the ratio of the widths $G_\ell(E)$ does not depend on $\rho_{\rm sn}(E)$. As a result, the partial probability of the compound nucleus formation $P_\ell(E)$ and the compound nucleus cross section (4) do not link to $\rho_{\rm sn}(E)$. Due to these, the properties of $\rho_{\rm sn}(E)$ are not discussed and it is possible to discuss results obtained in the model.

III. DISCUSSION

To start, it is useful to consider the probability of the compound nucleus formation qualitatively.

A. Qualitative consideration

Taking into account that the level density exponentially depends on the excitation energy and neglecting other energy dependencies of the level density, the width $\Gamma_\ell^{\rm qe}(E)$ can be approximated as

$$\Gamma_\ell^{\rm qe}(E) \propto \frac{\rho_{A_1}(\varepsilon_1)\rho_{A_2}(\varepsilon_2)}{2\pi\,\rho_{\rm sn}(E)}. \tag{46}$$

Here the energies ε_i are calculated by solving the system of equations

$$T^2 = \varepsilon_1/a_{A_1}(\varepsilon_1) = \varepsilon_2/a_{A_2}(\varepsilon_2), \tag{47}$$

$$\varepsilon_1 + \varepsilon_2 = E - B_\ell^{\rm qe}, \tag{48}$$

which leads to the same value of temperature T of both nuclei.

Applying the proposal used for getting Eq. (46) and in the case $B^{\rm ld} \gg B^{\rm sh}$, the width $\Gamma_\ell^{\rm cn}(E)$ can be approximated as

$$\Gamma_\ell^{\rm cn}(E) \propto \frac{\rho_A(\varepsilon_{\rm m})}{2\pi\,\rho_{\rm sn}(E)}. \tag{49}$$

Here the energy $\varepsilon_{\rm m}$ is coupled to the compound nucleus formation barrier value; see Eq. (13).

Substituting Eqs. (46) and (49) in (8), the expression for the ratio of the widths can be written in the simple form

$$G_\ell(E) \propto \frac{\rho_{A_1}(\varepsilon_1)\rho_{A_2}(\varepsilon_2)}{\rho_A(\varepsilon_{\rm m})}. \tag{50}$$

The energy level densities in Eq. (50) depend on the compound nucleus formation barrier $B^{\rm cnf} - Q$ [see Eq. (21)] and the quasielastic barrier $B_\ell^{\rm qe}$, which can be approximated as

$$B_\ell^{\rm qe} = B^{\rm qe} + \frac{\hbar^2\ell(\ell+1)}{2J^{\rm qe}}. \tag{51}$$

Here $B^{\rm qe}$ is the quasielastic barrier height for $\ell = 0$ and $J^{\rm qe} = \mu r_{\rm qe}^2$ is the moment of inertia of the two deformed nuclei at the quasielastic barrier. The barrier heights $B^{\rm cnf} - Q$ and $B_\ell^{\rm qe}$ are defined relatively as the interaction energies of incident nuclei at infinite distance between them.

Any shell effects are negligible in the case of large collision energies. Taking into account that the level density exponentially depends on the excitation energy and neglecting other energy dependencies, the energy level densities in Eq. (50) can be approximated as

$$\rho_{A_1}(\varepsilon_1)\rho_{A_2}(\varepsilon_2) \propto e^{2\sqrt{(a_{A_1}^0 + a_{A_2}^0)[E - B^{\rm qe} - \frac{\hbar^2\ell(\ell+1)}{2J^{\rm qe}}]}}, \tag{52}$$

$$\rho_A(\varepsilon_{\rm m}) \propto e^{2\sqrt{a_A^0\left[E+Q-B^{\rm ld}-\frac{\hbar^2\ell(\ell+1)}{2J^{\rm cnf}}\right]}}. \tag{53}$$

Here Eqs. (21), (47), (48), and (51) have been used.

Substituting the asymptotic level density parameters with $a_A^0 \approx A/10\ {\rm MeV}^{-1}$ and $a_{A_1}^0 + a_{A_2}^0 \approx A/10\ {\rm MeV}^{-1}$, and using Eqs. (52) and (53), the ratio of densities is given in the simple form

$$G_\ell(E) \propto \exp\left(2\sqrt{A/10}\ g_\ell\right). \tag{54}$$

Here

$$g_\ell(E) = \sqrt{E - B^{\rm qe} - \frac{\hbar^2\ell(\ell+1)}{2J^{\rm qe}}} - \sqrt{E - (B^{\rm ld} - Q) - \frac{\hbar^2\ell(\ell+1)}{2J^{\rm cnf}}}. \tag{55}$$

The values of the moments of inertia in this expression obey the inequality $J^{\rm qe} > J^{\rm cnf}$. Therefore, $\frac{\hbar^2\ell(\ell+1)}{2J^{\rm cnf}} > \frac{\hbar^2\ell(\ell+1)}{2J^{\rm qe}}$.

For the collision of heavy nuclei $\sqrt{A/10} \gtrsim 1$. The values of $g_\ell(E)$ depend on the values $B^{\rm ld} - Q$ and $B^{\rm qe}$. Thus, it is useful to consider two different cases, $B^{\rm ld} - Q < B^{\rm qe}$ and $B^{\rm ld} - Q > B^{\rm qe}$, separately.

1. The case $B^{\rm ld} - Q < B^{\rm qe}$

This case takes place for a light nucleus-nucleus system, for example $^{28}{\rm Si} + {}^{28}{\rm Si} \to {}^{56}{\rm Ni}$; see Table I. In the case $B^{\rm ld} - Q < B^{\rm qe}$ the values of $E - B^{\rm qe} - \frac{\hbar^2\ell(\ell+1)}{2J^{\rm qe}} < E - (B^{\rm ld} - Q) - \frac{\hbar^2\ell(\ell+1)}{2J^{\rm cnf}}$ and $g_\ell(E) \lesssim -1$ for small values of ℓ. At $g_\ell(E) \lesssim -1$ the values of $G_\ell(E) \ll 1$ and $P_\ell(E) = 1/[1 + G_\ell(E)] \approx 1$. As a result, the partial wave cross section of the compound-nucleus formation linearly increases with ℓ according to the law $\sigma_\ell^{\rm cn}(E) \approx \frac{\pi\hbar^2}{2\mu E}(2l+1)T_\ell(E)$ for small values of ℓ because $T_\ell(E) \approx 1$ at high collision energies E; see Fig. 1. The values of the cross sections $\sigma_\ell^{\rm cn}(E)$ and $\sigma_\ell^{\rm c}(E)$ are very close in this case; see Fig. 1.

However, even in the case $B^{\rm ld} - Q < B^{\rm qe}$ at very high values of ℓ, it may be that $E - B^{\rm qe} - \frac{\hbar^2\ell(\ell+1)}{2J^{\rm qe}} > E - (B^{\rm ld} - Q) - \frac{\hbar^2\ell(\ell+1)}{2J^{\rm cnf}}$ because of $\frac{\hbar^2\ell(\ell+1)}{2J^{\rm cnf}} > \frac{\hbar^2\ell(\ell+1)}{2J^{\rm qe}}$. In this case the values of $g_\ell(E) \gtrsim 1$, therefore, $G_\ell(E) \gg 1$, $P_\ell(E) \ll 1$,

TABLE I. The model values of the total compound nucleus formation barrier $B^{\rm cnf} - Q$, the liquid-drop part of the compound nucleus formation barrier $B^{\rm ld}$, the quasielastic barrier $B^{\rm qe}$, and the capture barrier for spherical incident nuclei $B^{\rm sph}$. The values of the liquid-drop fission barrier were obtained for symmetric fission $B^{\rm ld}_{\rm sym}$ applying the code BARFIT [100], the Q value of the compound nucleus formation reaction was obtained using [120], as was as the quadrupole deformation parameter at the compound nucleus formation barrier $\beta_{\rm cnf}$ used in the model. The values of barriers are presented for $\ell = 0$. All values of the barriers and Q value are given in MeV.

Comp. nucleus	^{56}Ni	^{149}Tb[a]	^{149}Tb[b]	^{161}Tm	^{162}Er	^{258}Rf
$B^{\rm cnf} - Q$	24.2	106.1	90.5	96.8	80.9	175.8
$B^{\rm ld} - Q$	20.2	105.6	90.0	95.9	79.3	169.5
$B^{\rm ld}$	31.1	27.4	37.7	33.2	31.9	0.0
$B^{\rm ld}_{\rm sym}$	31.1	27.4	27.4	24.2	26.4	0.6
$B^{\rm qe}$	27.3	105.5	90.3	93.9	80.5	165.3
$B^{\rm sph}$	27.9	112.2	95.9	99.7	84.2	177.8
$-Q$	−10.9	78.2	52.3	62.7	47.4	169.5
$\beta_{\rm cnf}$	1.28	1.95	1.59	1.50	0.54	0.45

[a]For reaction ^{84}Kr + ^{65}Cu → ^{149}Tb.
[b]For reaction ^{40}Ar + ^{109}Ag → ^{149}Tb.

and $\sigma^{\rm cn}_\ell(E) \ll \frac{\pi\hbar^2}{2\mu E}(2l+1)$ at high collision energy when $T_\ell(E) \approx 1$. As a result, $\sigma^{\rm cn}_\ell(E)$ and $P_\ell(E)$ exponentially decrease with increase of ℓ due to dependence of $G_\ell(E)$ on ℓ. This leads to $\sigma^{\rm cn}_\ell(E) \ll \sigma^{\rm c}_\ell(E)$. These conclusions agree with the numerical calculation results for the reaction ^{28}Si + ^{28}Si → ^{56}Ni presented in Fig. 1, where see that $\sigma^{\rm cn}_\ell(E) \ll \sigma^{\rm c}_\ell(E)$ for large values of ℓ.

Consequently, in the case $B^{\rm ld} - Q < B^{\rm qe}$ there is the critical value of the angular momentum $\ell_{\rm cr}(E)$, where the probabilities of the compound nucleus formation obey to the conditions

$$P_{\ell_{\rm cr}(E)-1}(E) \geqslant \tfrac{1}{2}, \quad P_{\ell_{\rm cr}(E)}(E) \leqslant \tfrac{1}{2}. \tag{56}$$

The values of $g_\ell(E)$ is around zero at ℓ around $\ell_{\rm cr}(E)$.

If $\ell \lesssim \ell_{\rm cr}(E)$ then $\sigma^{\rm cn}_\ell(E) \propto \frac{\pi\hbar^2}{2\mu E}(2l+1)T_\ell(E) \approx \sigma^{\rm c}_\ell(E)$ and the compound nucleus is formed at such values of ℓ in nucleus-nucleus collision without suppression because $P_\ell(E)$ is very close to 1; see Fig. 1. In comparison to this, at $\ell \gtrsim \ell_{\rm cr}(E)$ the values of $\sigma^{\rm cn}_\ell(E)$ exponentially decrease with the increase of ℓ and the compound nucleus formation is suppressed, i.e., $\sigma^{\rm cn}_\ell(E) \ll \sigma^{\rm c}_\ell(E)$; see Fig. 1. The partial quasielastic cross sections $\sigma^{\rm qe}_\ell(E)$ reach the maximal values $\sigma^{\rm qe}_\ell(E) = \frac{\pi\hbar^2}{2\mu E}(2\ell+1)T_\ell(E) \approx \sigma^{\rm c}_\ell(E)$ at $\ell \gtrsim \ell_{\rm cr}(E)$. Here

$$\sigma^{\rm qe}(E) = \sigma^{\rm c}(E) - \sigma^{\rm cn}(E) = \sum_{\ell=0}^{\infty}\sigma^{\rm qe}_\ell(E)$$
$$= \frac{\pi\hbar^2}{2\mu E}\sum_{\ell=0}^{\infty}(2\ell+1)T_\ell(E)[1-P_\ell(E)] \tag{57}$$

is the quasielastic cross section, which is related to the decay of the stuck-together nuclei to the quasi-elastic channel and other scattered channels; see the discussion after Eq. (7).

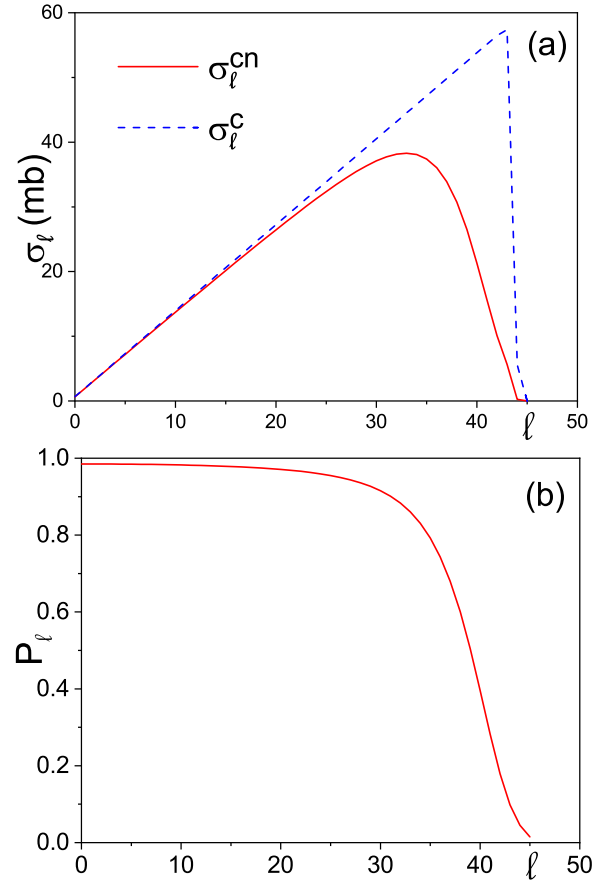

FIG. 1. (a) The dependencies of the capture $\sigma^{\rm c}_\ell(E)$ and compound nucleus formation $\sigma^{\rm cn}_\ell(E)$ partial cross sections on ℓ for the reaction ^{28}Si + ^{28}Si → ^{56}Ni at collision energy $E = 70$ MeV. (b) The dependence of the probability of the compound-nucleus formation P_ℓ on ℓ for the same reaction and collision energy as in (a).

Therefore, the compound-nucleus formation is defined by the competition between the decay branches of stuck-together nuclei related to the passage through the compound-nucleus formation barrier and the quasielastic barrier in the present model. The competition between the decay branches depends on the value of ℓ and changes significantly at $\ell = \ell_{\rm cr}$ in the case $B^{\rm ld} - Q < B^{\rm qe}$.

The dependence of $\ell_{\rm cr}(E)$ for the reaction ^{28}Si + ^{28}Si → ^{56}Ni is presented in Fig. 2. The value of $\ell_{\rm cr}(E)$ is calculated according to the conditions (56). The increase of $\ell_{\rm cr}(E)$ with rising E at $E \lesssim 100$ MeV is related to the increasing value of $E - B^{\rm qe} - \frac{\hbar^2\ell(\ell+1)}{2J^{\rm qe}}$ with E. The asymptotic level density parameters linked to the quasielastic barrier and compound nucleus formation barrier satisfy the condition $a^0_{A_1} + a^0_{A_2} > a^0_A$ due to the term $A^{2/3}$; see Eq. (16). As a result, the values $\ell_{\rm cr}(E)$ decrease with rising E at $E \gtrsim 130$ MeV and $\ell_{\rm cr}(E) = 0$ for very high energies $E \gtrsim 340$ MeV; see Fig. 2. Note that $\ell_{\rm cr}(E) = 0$ for $P_{\ell=0}(E) \leqslant \frac{1}{2}$.

The maximal value of the critical value of the angular momentum $\ell_{\rm cr}(E)$ obtained in the present model for the reaction ^{28}Si + ^{28}Si → ^{56}Ni is slightly higher than the values of the critical angular momentum related to the instability

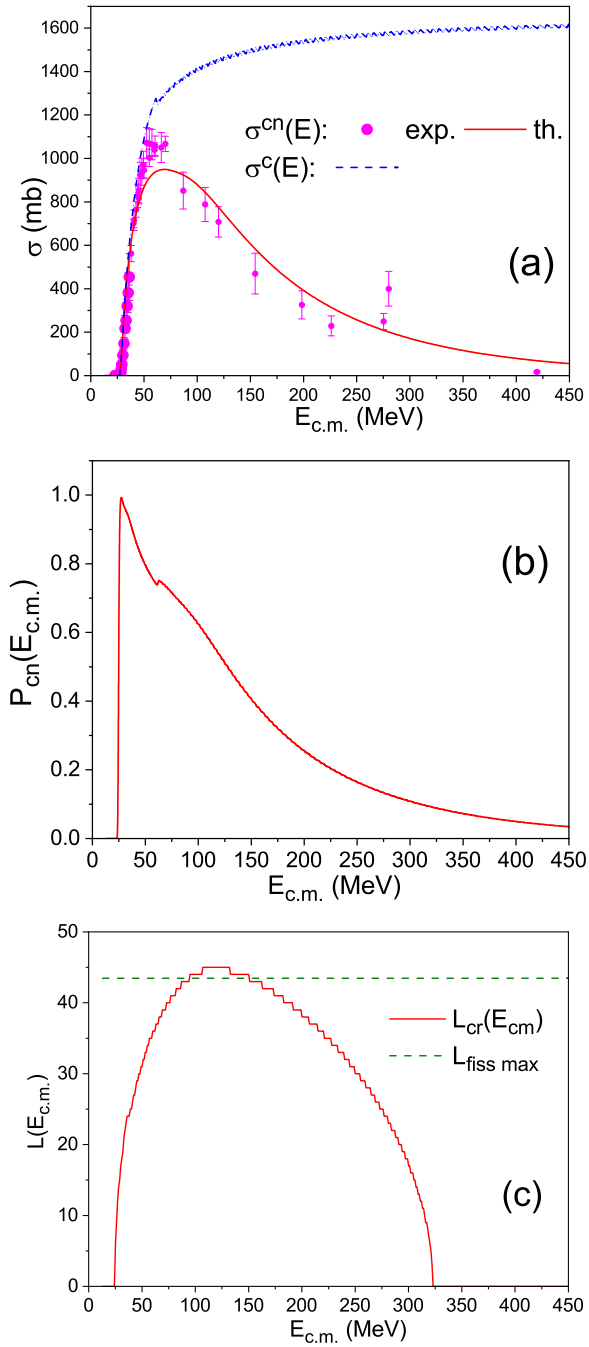

FIG. 2. (a) The dependencies of the capture $\sigma^{c}(E)$ and compound nucleus formation $\sigma^{cn}(E)$ cross sections on E for the reaction $^{28}\mathrm{Si}+{}^{28}\mathrm{Si}\rightarrow{}^{56}\mathrm{Ni}$. The experimental data for the compound-nucleus formation cross-section are taken from Refs. [123–129]. (b) The dependence of the total probability of the compound nucleus formation $P(E)$ on E for the same reaction as in (a). (c) The dependence of the critical angular momentum $\ell_{cr}(E)$ on E for the same reaction as in (a). $L_{\mathrm{fiss\ max}}$ is the value of the critical angular momentum related to the instability of the nucleus against prompt fission evaluated with the code BARFIT [100].

of the nucleus ^{56}Ni against prompt fission, $L_{\mathrm{fiss\ max}}$, which is calculated using the code BARFIT [100]; see Fig. 2. However, the values $L_{\mathrm{fiss\ max}}$ and the liquid-drop fission barrier are evaluated in the code BARFIT using interpolation formulas, which lead to errors [100]. Besides this, the values of the fission barrier and $L_{\mathrm{fiss\ max}}$ depend on the parameter values of the liquid-drop model, which change with time (compare the parameter values of the liquid-drop model used in Refs. [98,100]). For example, the small changes in the value of the surface tension coefficient lead to noticeable changes in the values of the liquid-drop barrier and $L_{\mathrm{fiss\ max}}$. Therefore, it is possible to conclude that the maximal value of $\ell_{cr}(E)$ obtained in the model agrees excellently with the value of $L_{\mathrm{fiss\ max}}$; see Fig. 2. This confirms that the value of β_{cnf}, which is obtained by fitting the experimental data for the compound nucleus cross section (see Table I), is reliable. (Here and below the fitting of the experimental data is made by eye.) At larger value of β_{cnf}, the value of J_{cnf} approaches the value of J_{qe}. Due to this, the strong competition between the compound nucleus formation and quasielastic processes starts from higher values of ℓ, and $\ell_{cr}(E)$ rises with an increase of β_{cnf}.

Note that the critical value of the angular momentum, ℓ_{cr}, is widely applied in the various models of the compound nucleus formation in heavy-ion reactions; see, for example, Refs. [1,2,52,53] and papers cited therein. In contrast to the proposed model, the physical interpretation of the nature of the critical angular momentum in Ref. [53] was related to the instability of the nucleus against prompt fission, i.e., it was linked to the value $L_{\mathrm{fiss\ max}}$. Besides this, the critical value of the angular momentum and $L_{\mathrm{fiss\ max}}$ are independent of E in Refs. [52,53].

2. *The case $B^{\mathrm{ld}}-Q>B^{\mathrm{qe}}$*

This case may take place for the collisions of heavy nuclei; see Table I. The values of $B^{\mathrm{ld}}-Q$ are significantly larger than B^{qe} for reactions used in the synthesis of the superheavy elements.

In the case $B^{\mathrm{ld}}-Q>B^{\mathrm{qe}}$, the value of $g_{\ell}(E)<0$. As a result, $G_0(E)\gtrsim 1$ and the value $G_{\ell}(E)$ rises with increasingℓ. If $G_{\ell}>1$ then $G_{\ell}(E)\gg 1$ and $P_{\ell}(E)\ll 1$, i.e., the formation of a compound nucleus is strongly suppressed. The values $P_{\ell}(E)\ll 1$ for any value of ℓ for the reaction $^{40}\mathrm{Ar}+{}^{121}\mathrm{Sb}\rightarrow{}^{161}\mathrm{Tm}$; see Fig. 3. Therefore, the values of the partial compound nucleus formation cross section $\sigma^{cn}_{\ell}(E)$ for this reaction are much smaller than the partial capture cross sections $\sigma^{c}_{\ell}(E)$ in this case too; see Fig. 3. The values of quasielastic cross section $\sigma^{qe}(E)$ are high in this case and close to $\sigma^{c}(E)$.

B. Cross sections for a light nucleus-nucleus system

The dependencies of the cross sections of the capture, $\sigma^{c}(E)$, and compound nucleus formation, $\sigma^{cn}(E)$, on E for the reaction $^{28}\mathrm{Si}+{}^{28}\mathrm{Si}\rightarrow{}^{56}\mathrm{Ni}$ are presented in Fig. 2. The values of the compound-nucleus formation cross section calculated in the model agree well with available experimental data [123–129]. The values of $\sigma^{c}(E)$ are much higher than the values of $\sigma^{cn}(E)$. $\sigma^{c}(E)$ always rises with an increase in collision energy E. In comparison to this, $\sigma^{cn}(E)$ increases at sub-barrier collision energies; however, it decreases at high collision energy due to the competition between the compound-nucleus formation and quasielastic processes.

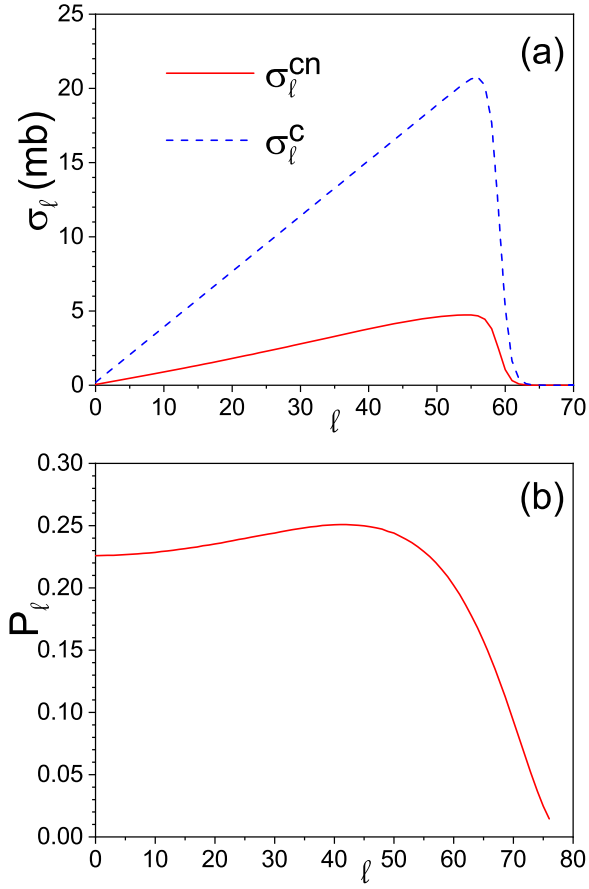

FIG. 3. (a) The dependencies of the capture $\sigma_\ell^{c}(E)$ and compound nucleus formation $\sigma_\ell^{cn}(E)$ partial cross sections on ℓ for the reaction $^{40}\mathrm{Ar}+{}^{121}\mathrm{Sb}\to{}^{161}\mathrm{Tm}$ at $E=116$ MeV. (b) The dependence of the probability of the compound-nucleus formation P_ℓ on ℓ for the same reaction and collision energy as in (a).

The dependence of the total compound-nucleus formation probability $P(E)$ on E for the reaction $^{28}\mathrm{Si}+{}^{28}\mathrm{Si}\to{}^{56}\mathrm{Ni}$ is presented in Fig. 2 too. $P(E)$ values decrease with E at above-barrier collision energies.

The quasielastic barrier is slightly lower than the capture barrier B^{sph}, which takes place for the incident spherical nuclei; see Table I. Therefore, the probability of the elastic decay of the stuck-together nuclei is low.

For the sake of a better description of the compound nucleus formation cross section, the radius parameters of the nuclear part of the nucleus-nucleus potential, R_{0i}, are slightly modified $R_{0i}+\delta_{Ri}$. The values of δ_{Ri} are given in Table II. The radius value variation modulates the coupling channel effects on the heavy-ion fusion, which are important around the barrier [53].

As pointed out earlier, the probability of compound nucleus formation depends on the competition between transitions over the compound nucleus formation barrier and the quasielastic barrier. The compound nucleus formation barrier height consists of the liquid-drop and shell-corrections contributions; see Eqs. (20) and (21). The height of the liquid-drop part of the compound nucleus formation barrier, B^{ld}, is given in Table I. Due to symmetry in the incident channel of the reaction $^{28}\mathrm{Si}+{}^{28}\mathrm{Si}\to{}^{56}\mathrm{Ni}$, the value B^{ld} used in the model calculation coincides with the value of the liquid-drop fission barrier for symmetric fission, $B^{\mathrm{ld}}_{\mathrm{sym}}$, of the nucleus ^{56}Ni obtained using the code BARFIT [100]. Note that symmetric fission is a feature of the liquid-drop model. The value $B^{\mathrm{ld}}=B^{\mathrm{ld}}_{\mathrm{sym}}$ leads to a good description of the experimental data for the reaction $^{28}\mathrm{Si}+{}^{28}\mathrm{Si}\to{}^{56}\mathrm{N}$ in the model.

TABLE II. The values of δ_{Ri} used for fitting the experimental cross section data.

	Nucleus				
	^{28}Si	^{30}Si	^{40}Ar	^{50}Ti	^{65}Cu
δ_{Ri} (fm)	0.1	0.27	0.2	0.35	0.4
	^{84}Kr	^{109}Ag	^{121}Sc	^{132}Xe	^{208}Pb
δ_{Ri} (fm)	0.4	0.2	0.5	0.27	0.35

C. Cross sections for heavy nucleus-nucleus systems

The comparison of the dependencies of the cross sections of the capture, $\sigma^{\mathrm{c}}(E)$, and compound nucleus formation, $\sigma^{\mathrm{cn}}(E)$, on the collision energy in the center-of-mass E with the available experimental data [132,133] for reactions $^{84}\mathrm{Kr}+{}^{65}\mathrm{Cu}\to{}^{149}\mathrm{Tb}$, $^{40}\mathrm{Ar}+{}^{109}\mathrm{Ag}\to{}^{149}\mathrm{Tb}$, $^{40}\mathrm{Ar}+{}^{121}\mathrm{Sb}\to{}^{161}\mathrm{Tm}$, and $^{132}\mathrm{Xe}+{}^{30}\mathrm{Si}\to{}^{162}\mathrm{Er}$ is presented in Fig. 4. The experimental data are well described in the present model.

The systems considered now are much heavier than the system $^{28}\mathrm{Si}+{}^{28}\mathrm{Si}\to{}^{56}\mathrm{Ni}$ considered early. In comparison to the light system, the height of the compound nucleus formation barrier $B^{\mathrm{cnf}}-Q$ is slightly higher than the height of the quasielastic barrier B^{qe} for heavy systems; see Table I. Due to the strong competition between the compound nucleus formation and the quasielastic decay of the stuck-together nuclei in the case $B^{\mathrm{cnf}}-Q>B^{\mathrm{qe}}$, the partial $P_\ell(E)$ probability of compound nucleus formation is noticeably smaller than 1 for all values of ℓ; see Fig. 3. As a result, the partial cross section of the compound nucleus formation is significantly smaller than the capture cross section; see, for example, Fig. 3. This leads to the total probability of compound nucleus formation being remarkably smaller than 1, and the values of compound-nucleus formation cross section $\sigma^{\mathrm{cn}}(E)$ are seriously smaller than the capture cross section $\sigma^{\mathrm{c}}(E)$ for energies larger than the barrier; see Fig. 4.

For the sake of a good description of $\sigma^{\mathrm{c}}(E)$, the radius parameters of the nuclear part of the nucleus-nucleus potential, R_{0i}, are modified as $R_{0i}+\delta_{Ri}$. The values of δ_{Ri} for the considered incident nuclei are given in Table II.

The heights of the liquid-drop part of the compound nucleus formation barrier B^{ld} for reactions $^{84}\mathrm{Kr}+{}^{65}\mathrm{Cu}\to{}^{149}\mathrm{Tb}$, $^{40}\mathrm{Ar}+{}^{109}\mathrm{Ag}\to{}^{149}\mathrm{Tb}$, $^{40}\mathrm{Ar}+{}^{121}\mathrm{Sb}\to{}^{161}\mathrm{Tm}$, and $^{132}\mathrm{Xe}+{}^{30}\mathrm{Si}\to{}^{162}\mathrm{Er}$ are given in Table I. For the near symmetric reaction $^{84}\mathrm{Kr}+{}^{65}\mathrm{Cu}\to{}^{149}\mathrm{Tb}$, the value B^{ld} used in the calculations coincides with the value of the liquid-drop fission barrier $B^{\mathrm{ld}}_{\mathrm{sym}}$ obtained using the code BARFIT [100].

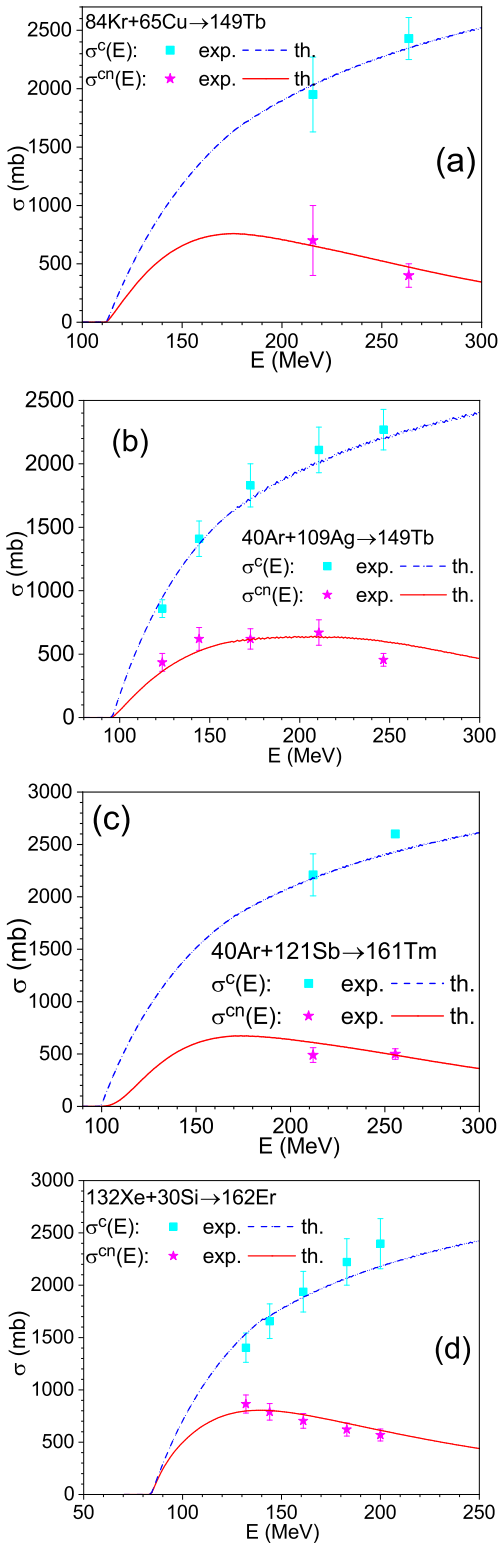

FIG. 4. The comparison of the capture $\sigma^{c}(E)$ and compound nucleus formation $\sigma^{cn}(E)$ cross sections calculated in the model for the reactions $^{84}\mathrm{Kr}+{}^{65}\mathrm{Cu}\rightarrow{}^{149}\mathrm{Tb}$ (a), $^{40}\mathrm{Ar}+{}^{109}\mathrm{Ag}\rightarrow{}^{149}\mathrm{Tb}$ (b), $^{40}\mathrm{Ar}+{}^{121}\mathrm{Sb}\rightarrow{}^{161}\mathrm{Tm}$ (c), and $^{132}\mathrm{Xe}+{}^{30}\mathrm{Si}\rightarrow{}^{162}\mathrm{Er}$ (d) with the experimental data [132,133].

For strongly asymmetric reactions $^{40}\mathrm{Ar}+{}^{109}\mathrm{Ag}\rightarrow{}^{149}\mathrm{Tb}$, $^{40}\mathrm{Ar}+{}^{121}\mathrm{Sb}\rightarrow{}^{161}\mathrm{Tm}$, and $^{132}\mathrm{Xe}+{}^{30}\mathrm{Si}\rightarrow{}^{162}\mathrm{Er}$, the values of B^{ld} are higher than B^{ld}_{sym}; see Table I. This is related to the left-right asymmetric shapes of the nuclear system along the trajectory of the compound nucleus formation from the stuck-together nuclei. The process of compound nucleus formation in the asymmetric reaction is somehow inverse to the cluster emission process. The cluster emission is a strongly asymmetric fission [130,131]. The ordinary fission barrier height is much smaller than the cluster emission barrier height [71]. For example, the height of the ordinary fission barrier in $^{226}\mathrm{Ra}$ calculated relative to the ground state of the fissioning nucleus is 8.2 MeV [101] while the barrier heights related to the emission of clusters $^{14}\mathrm{C}$ or $^{20}\mathrm{O}$ from $^{226}\mathrm{Ra}$ are over 30 MeV [134]. Therefore, the high values of B^{ld} given in Table I for asymmetric reactions are reasonable. These values of B^{ld} are obtained by fitting the experimental data for the compound nucleus formation cross section.

The value of the compound nucleus formation cross section depends on the moment of inertia of the nucleus at the compound nucleus formation barrier J^{cnf}. J^{cnf} links to the value of the quadrupole deformation parameter in the barrier saddle point, β_{cnf}. The values of β_{cnf} in the model are taken by fitting the compound nucleus formation cross section. The used values of β_{cnf} are given in Table I.

Note that two different values of β_{cnf} for $^{149}\mathrm{Tb}$ are given in Table I because the trajectories of the compound nucleus formation in reactions $^{84}\mathrm{Kr}+{}^{65}\mathrm{Cu}\rightarrow{}^{149}\mathrm{Tb}$ and $^{40}\mathrm{Ar}+{}^{109}\mathrm{Ag}\rightarrow{}^{149}\mathrm{Tb}$ are different. The different trajectories have different positions of the barrier point and, therefore, different values of β_{cnf}. The effect of both different barrier values and different values of β_{cnf} can be seen in Fig. 4 by comparing the results for the reactions $^{84}\mathrm{Kr}+{}^{65}\mathrm{Cu}\rightarrow{}^{149}\mathrm{Tb}$ and $^{40}\mathrm{Ar}+{}^{109}\mathrm{Ag}\rightarrow{}^{149}\mathrm{Tb}$ leading to the same compound nucleus.

The quasielastic barrier is much lower than the capture barrier B^{sph} for heavy systems; see Table I. Therefore, the probability of the elastic decay of the stuck-together nuclei is very low.

D. Cross sections for a super-heavy nucleus-nucleus system

The model dependencies of the cross sections of the capture, $\sigma^{c}(E)$, and compound nucleus formation, $\sigma^{cn}(E)$, as well as the total probability of compound nucleus formation, $P(E)$, on the collision energy E for the reaction $^{50}\mathrm{Ti}+{}^{208}\mathrm{Pb}\rightarrow{}^{258}\mathrm{Rf}$ are compared with the available experimental data [20,22,24,135,136] in Fig. 5. The experimental data for $\sigma^{cn}(E)$ are well described in the present model. The model values of $P(E)$ are very close to experimental data at low collision energies and are twice higher than the experimental data at high collision energy; see Fig. 5. Unfortunately, the experimental data for $\sigma^{cn}(E)$ and $P(E)$ measured by different groups are not very consistent. Note that there are no experimental data for $\sigma^{c}(E)$ for this reaction.

The height of the compound nucleus formation barrier B^{cnf} is much greater than the height of the quasielastic barrier B^{qe} for reactions leading to superheavy systems; see Table I. Therefore, the formation of a compound nucleus for such a heavy system is strongly suppressed. This is seen in Fig. 5 at low collision energies when the collision energies are close

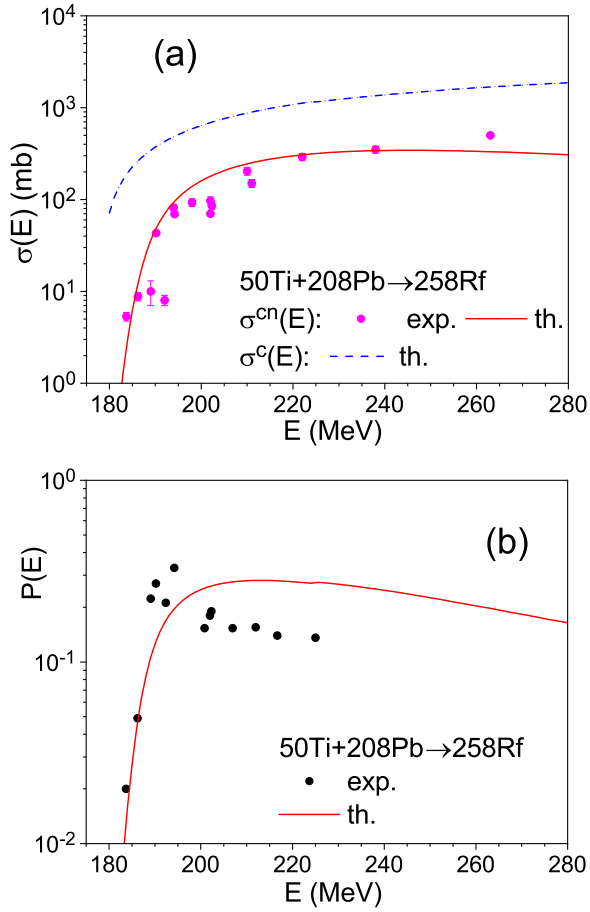

FIG. 5. (a) The dependencies of the capture $\sigma^{c}(E)$ and compound nucleus formation $\sigma^{cn}(E)$ cross sections on the collision energy E for the reaction $^{50}\mathrm{Ti}+{}^{208}\mathrm{Pb}\rightarrow{}^{258}\mathrm{Rf}$. The experimental data are taken from Refs. [20,22,24,135,136]. (b) The dependence of the total probability of the compound-nucleus formation, $P(E)$, on the collision energy E for the same reaction as in (a). The experimental data are taken from Refs. [20,135,136].

to the compound nucleus formation barrier and competition between these processes is very strong.

The model calculations of the cross sections and compound nucleus formation probability for reaction $^{50}\mathrm{Ti}+{}^{208}\mathrm{Pb}\rightarrow{}^{258}\mathrm{Rf}$ are done for the values of parameters given in Tables I and II. Most of the parameters for this reaction have values similar to the ones for other reactions.

Note that the value of β_{cnf} for the ^{258}Rf case is smaller than the ones for other systems; see Table I. Note that the values of the quadrupole deformation parameter of the nuclear shape in the fission barrier point smoothly decrease with increasing mass A and charge Z of the fissioning nuclei in the liquid-drop model; see, for example, Ref. [100]. Therefore, the fission barrier saddle points in super- and ultraheavy elements occur at small values of the quadrupole deformation parameter [99,137]. The same tendency should occur for the compound nucleus formation barrier. Therefore the small value of β_{cnf} for this reaction is natural.

The value of the total fission barrier height for ^{258}Rf obtained in Ref. [101] is used in the present calculation. The value B^{ld} used for fitting is given in Table I. Note that the heights of barriers of the fission and cluster emission are close for superheavy nuclei [138,139]. Therefore, the value of the compound nucleus formation barrier height for reaction $^{50}\mathrm{Ti}+{}^{208}\mathrm{Pb}\rightarrow{}^{258}\mathrm{Rf}$ given in Table I is well supported.

E. Compound nucleus formation in symmetric nucleus-nucleus collisions

It is useful to consider the compound nucleus formation in symmetric nucleus-nucleus reactions $^{A}Z+{}^{A}Z\rightarrow{}^{2A}2Z$, when the incident nuclei ^{A}Z with Z protons and A nucleons are located around the beta-stability line. Let the incident spherical or almost spherical nuclei belong to the range from ^{20}Ne to ^{123}Sb. Then the compound nuclei lie in the range from ^{40}Ca to ^{246}No.

As pointed out earlier, the compound nucleus formation barrier $B^{\mathrm{cfn}}(0)$ for a symmetric incident system is close to the fission barrier of this nucleus. Therefore, $B^{\mathrm{cfn}}(0)=B^{\mathrm{ld}}-E^{\mathrm{gs\ sh}}$, where the values B^{ld} can be found using the code BARFIT [100]. Recall that the values $E^{\mathrm{gs\ sh}}$ are taken from Ref. [98]. The values of $B^{\mathrm{cfn}}(0)$ for $\ell=0$ does not depend on β_{cnf}.

Recall that the value of barrier $B^{\mathrm{cfn}}(0)$ is calculated relative to the ground state energy of the compound nucleus. The height of this barrier evaluated relative to the interaction energy of the incident nuclei at infinite distance between them is $B^{\mathrm{cfn}}(0)-Q$. The barrier height B^{qe} is defined relative to the interaction energy of the incident nuclei at infinite distance between them too.

The dependencies of the difference $B^{\mathrm{qe}}-B^{\mathrm{cfn}}(0)+Q$ and the partial probability of the compound nucleus formation $P_0^{\mathrm{cn}}(E)$ for $\ell=0$ on the number of protons in incident nucleus Z for symmetric reactions $^{A}Z+{}^{A}Z\rightarrow{}^{2A}2Z$ are presented in Fig. 6. The calculations are done for stable or near-stable isotopes ^{A}Z around the beta-stability line, therefore there are several dots for a fixed value of Z in Fig. 6. The dependence $P_0^{\mathrm{cn}}(E)$ is presented in Fig. 6 in linear and logarithmic scales because they give complementary information. The values B^{sph} are calculated using $\delta_R=0$ because this value of δ_R leads to the best description of the empirical nucleus-nucleus interaction barrier heights for different collision systems [112]. The values of $P_0^{\mathrm{cn}}(E)$ are calculated at the above-barrier collision energy $E=B^{\mathrm{sph}}+10$ MeV.

The values of the difference $B^{\mathrm{qe}}-B^{\mathrm{cfn}}(0)+Q>1$ MeV for $Z\leqslant 41$ for most nuclear systems; see Fig. 6. For such values of Z the values $P_0^{\mathrm{cn}}(E)$ are very close to 1; see Fig. 6. Similar behavior has been observed in the reaction $^{28}\mathrm{Si}+{}^{28}\mathrm{Si}\rightarrow{}^{56}\mathrm{Ni}$. Note that the formation of the compound nucleus at high collision energies for such heavy ion systems is suppressed for higher values of ℓ.

The values of the difference $B^{\mathrm{qe}}-B^{\mathrm{cfn}}(0)+Q$ are around zero for the range $42\leqslant Z\leqslant 45$; see Fig. 6. For this interval of Z the values $P_0^{\mathrm{cn}}(E)$ are in the range from 0.1 to 1. Analogous values of $P_0^{\mathrm{cn}}(E)$ are observed in heavy collision systems; see Sec. III C.

The values of the difference $B^{\mathrm{qe}}-B^{\mathrm{cfn}}(0)+Q<0$ for $Z\geqslant 46$ and the values $P_0^{\mathrm{cn}}(E)\ll 0.1$ for most nuclear systems; see Fig. 6. This situation is the same as for the

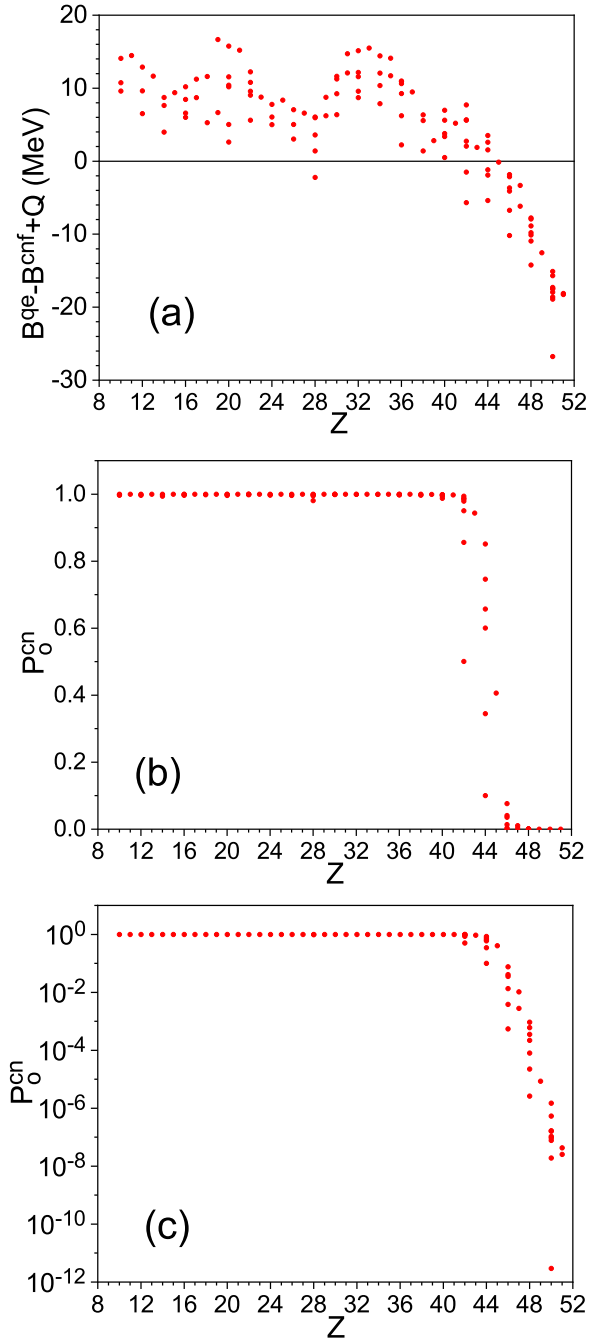

FIG. 6. (a) The dependence of the difference $B^{\rm qe} - B^{\rm cfn}(0)$ on the number of protons Z in incident nuclei for the symmetric reactions ${}^{A}Z + {}^{A}Z \to {}^{2A}2Z$. (b) The dependence of the probability $P_0^{\rm cn}$ of compound nucleus formation for $\ell = 0$ on the number of protons Z in incident nuclei in linear scale for the same reactions as in (a). (c) The same as in (b), but in logarithmic scale.

superheavy systems; see Sec. III D. The values of the difference $B^{\rm qe} - B^{\rm cfn}(0) + Q$ decrease strongly with rising charge of incident nuclei. As a result, the values of $P_0^{\rm cn}(E)$ drastically decrease with rising Z.

Due to strong changes of behavior of $P_0^{\rm cn}(E)$ in the range of Z from 40 to 46, it is interesting to discuss the reactions ${}^{90}{\rm Zr} + {}^{90}{\rm Zr} \to {}^{180}{\rm Hg}$, ${}^{100}{\rm Mo} + {}^{100}{\rm Mo} \to {}^{200}{\rm Po}$, and ${}^{110}{\rm Pd} + {}^{110}{\rm Pd} \to {}^{220}{\rm U}$ in detail. Recall that the proton numbers Z in ${}^{90}{\rm Zr}$, ${}^{100}{\rm Mo}$, and ${}^{110}{\rm Pd}$ are 40, 42, and 46, respectively.

The analysis of the experimental data of the reaction ${}^{90}{\rm Zr} + {}^{90}{\rm Zr} \to {}^{180}{\rm Hg}$ shows that the total probability of the compound nucleus formation in this reaction at energies a little over the capture barrier is slightly smaller than 1 [5]. In the case of the reaction ${}^{100}{\rm Mo} + {}^{100}{\rm Mo} \to {}^{200}{\rm Po}$ the total compound nucleus formation probability is smaller than in the case of the reaction ${}^{90}{\rm Zr} + {}^{90}{\rm Zr} \to {}^{180}{\rm Hg}$. By comparing the compound nucleus formation cross sections for the reactions ${}^{90}{\rm Zr} + {}^{90}{\rm Zr} \to {}^{180}{\rm Hg}$, ${}^{100}{\rm Mo} + {}^{100}{\rm Mo} \to {}^{200}{\rm Po}$, and ${}^{110}{\rm Pd} + {}^{110}{\rm Pd} \to {}^{220}{\rm U}$ [5], one may conclude that the total probability of the compound nucleus formation for reaction ${}^{110}{\rm Pd} + {}^{110}{\rm Pd} \to {}^{220}{\rm U}$ is in the range 10^{-3}–10^{-6} depending on the collision energy. The behavior of $P_0^{\rm cn}(E)$ presented in Fig. 6 agrees with the discussed experimental tendency for the reactions ${}^{90}{\rm Zr} + {}^{90}{\rm Zr} \to {}^{180}{\rm Hg}$, ${}^{100}{\rm Mo} + {}^{100}{\rm Mo} \to {}^{200}{\rm Po}$, and ${}^{110}{\rm Pd} + {}^{110}{\rm Pd} \to {}^{220}{\rm U}$ observed in Ref. [5].

The formation of compound nuclei in symmetric reactions with incident nuclei heavier than ${}^{110}{\rm Pd}$ is strongly suppressed; see Fig. 6. Therefore, the cross sections of synthesis of superheavy nuclei in symmetric reactions are very small in the framework of the present model. This agrees with the results of experimental studies of the fusion reaction ${}^{136}{\rm Xe} + {}^{136}{\rm Xe}$ [27]. However, if the competition between the compound nucleus formation and the quasielastic decay of the stuck-together nuclei is neglected then the cross sections of synthesis of superheavy nuclei in symmetric reactions are much higher [32,33]. Therefore, this competition is very important for describing the compound nucleus formation for reactions leading to superheavy elements [39].

IV. CONCLUSION

A model for the calculation of the compound nucleus formation cross section and the probability of compound nucleus formation in heavy ion collisions is proposed. It is shown that the competition between the penetration through both the compound nucleus formation barrier and the quasielastic barrier is very important for the description of compound nucleus formation. This competition constrains the compound nucleus formation in collisions of light nuclei at high partial waves. For heavy and especially for superheavy compound nuclei in heavy-ion collisions, this competition strongly suppresses the compound nucleus formation for all partial waves.

A good description of the available experimental data for various reactions leading to light, heavy, and superheavy compound nuclei is obtained with the model. Therefore, the proposed mechanism of compound nucleus formation is a general feature of nuclear reactions with heavy ions.

The height of the compound nucleus formation barrier is lower than that of the quasielastic barrier for light nucleus-nucleus systems for low partial waves. In this case, the probability of compound nucleus formation is close to 1.

For heavy nucleus-nucleus systems, the compound nucleus formation barrier is slightly higher than the quasielastic

barrier. The compound nucleus formation barrier is much higher than the quasielastic barrier for systems leading to superheavy compound nuclei. The probability of compound nucleus formation is suppressed when the quasielastic barrier is lower than the compound nucleus formation barrier.

The height of the liquid-drop part of the compound nucleus formation barrier calculated relative to the ground state of the compound nucleus is very close to the fission barrier height of the liquid-drop model for incident symmetric or near-symmetric nucleus-nucleus systems. In comparison to this, the height of this barrier for strongly asymmetric incident nucleus-nucleus systems may be significantly greater than the liquid-drop fission barrier height because the liquid-drop fission barrier is related to symmetric fission.

ACKNOWLEDGMENTS

The author thanks the support of Professors Fabiana Gramegna, Enrico Fioretto, Giovanna Montagloli, and Alberto Stefanini. The author thanks for the support Istituto Nazionale di Fisica Nucleare, Laboratori Nazionali di Legnaro of Istituto Nazionale di Fisica Nucleare, the National Academy of Sciences of Ukraine, and Taras Shevchenko, the National University of Kiev.

[1] J. R. Birkelund *et al.*, Phys. Rep. **56**, 107 (1979).
[2] J. R. Birkelund and J. R. Huizenga, Annu. Rev. Nucl. Part. Sci. **33**, 265 (1983).
[3] R. A. Esterlund *et al.*, Nucl. Phys. A **435**, 597 (1985).
[4] W. Q. Shen *et al.*, Phys. Rev. C **36**, 115 (1987).
[5] K.-H. Schmidt and W. Morawek, Rep. Prog. Phys. **54**, 949 (1991).
[6] D. J. Hinde, M. Dasgupta, and A. Mukherjee, Phys. Rev. Lett. **89**, 282701 (2002).
[7] G. N. Knyazheva *et al.*, Phys. Rev. C **75**, 064602 (2007).
[8] R. Yanez, W. Loveland, J. S. Barrett, L. Yao, B. B. Back, S. Zhu, and T. L. Khoo, Phys. Rev. C **88**, 014606 (2013).
[9] R. du Rietz, E. Williams, D. J. Hinde, M. Dasgupta, M. Evers, C. J. Lin, D. H. Luong, C. Simenel, and A. Wakhle, Phys. Rev. C **88**, 054618 (2013).
[10] E. M. Kozulin *et al.*, Phys. Rev. C **96**, 064621 (2017).
[11] E. Vardaci *et al.*, J. Phys. G **46**, 103002 (2019).
[12] N. Kumar, D. C. Biswas, T. K. Ghosh, J. Sadhukhan, B. N. Joshi, Y. K. Gupta, R. P. Vind, G. K. Prajapati, S. Dubey, L. S. Danu, S. Mukhopadhyay, K. Mahata, B. V. John, and S. Sodaye, Phys. Rev. C **99**, 041602(R) (2019).
[13] E. M. Kozulin *et al.*, Phys. Rev. C **99**, 014616 (2019).
[14] E. M. Kozulin *et al.*, Phys. Lett. B **819**, 136442 (2021).
[15] D. J. Hinde, M. Dasgupta, and E. C. Simpson, Prog. Part. Nucl. Phys. **118**, 103856 (2021).
[16] A. Sen, T. K. Ghosh, E. M. Kozulin, I. M. Itkis, G. N. Knyazheva, K. V. Novikov, S. Bhattacharya, K. Banerjee, and C. Bhattacharya, Phys. Rev. C **105**, 014627 (2022).
[17] E. M. Kozulin *et al.*, Phys. Rev. C **105**, 024617 (2022).
[18] D. J. Hinde *et al.*, Phys. Rev. C **106**, 064614 (2022).
[19] T. Tanaka *et al.*, Phys. Rev. C **107**, 054601 (2023).
[20] R. S. Naik *et al.*, Phys. Rev. C **76**, 054604 (2007).
[21] E. M. Kozulin, G. N. Knyazheva, K. V. Novikov, I. M. Itkis, M. G. Itkis, S. N. Dmitriev, Y. T. Oganessian, A. A. Bogachev, N. I. Kozulina, I. Harca, W. H. Trzaska, and T. K. Ghosh, Phys. Rev. C **94**, 054613 (2016).
[22] K. Banerjee, D. J. Hinde, M. Dasgupta, E. C. Simpson, D. Y. Jeung, C. Simenel, B. M. A. Swinton-Bland, E. Williams, I. P. Carter, K. J. Cook, H. M. David, C. E. Dullmann, J. Khuyagbaatar, B. Kindler, B. Lommel, E. Prasad, C. Sengupta, J. F. Smith, K. Vo-Phuoc, J. Walshe, and A. Yakushev, Phys. Rev. Lett. **122**, 232503 (2019).
[23] K. Banerjee, Phys. Lett. B **820**, 136601 (2021).
[24] M. G. Itkis *et al.*, Eur. Phys. J. A **58**, 178 (2022).
[25] S. Hofmann, in *The Euroschool Lectures on Physics with Exotic Beams, Vol. III*, Lecture Notes in Physics Vol. 764 (Springer, Berlin, 2009), p. 203.
[26] Yu. Oganessian and V. K. Utyonkov, Rep. Prog. Phys. **78**, 036301 (2015).
[27] Yu. Oganessian *et al.*, Phys. Rev. C **79**, 024608 (2009).
[28] K. Morita, Nucl. Phys. A **944**, 30 (2015).
[29] Yu. Ts. Oganessian *et al.*, Phys. Rev. C **106**, L031301 (2022).
[30] Y. Aritomo, T. Wada, M. Ohta, and Y. Abe, Phys. Rev. C **59**, 796 (1999).
[31] V. Yu. Denisov and S. Hofmann, Phys. Rev. C **61**, 034606 (2000).
[32] V. Yu. Denisov. Denisov, Prog. Part. Nucl. Phys. **46**, 303 (2001).
[33] V. Yu. Denisov, in *Proceedings of the NATO Advanced Research Workshop on The Nuclear Many-Body Problem 2001*, Brijuni, Pula, Croatia (Kluwer Academic, Amsterdam, 2002), p. 305.
[34] V. V. Volkov, Fiz. Elem. Chastits At. Yadra **35**, 797 (2004) [Phys. Part. Nucl. **35**, 425 (2004)].
[35] M. Huang, Z. Gan, X. Zhou, J. Li, and W. Scheid, Phys. Rev. C **82**, 044614 (2010).
[36] L. Zhu, W.-J. Xie, and F.-S. Zhang, Phys. Rev. C **89**, 024615 (2014).
[37] S. Ayik, B. Yilmaz, and O. Yilmaz, Phys. Rev. C **92**, 064615 (2015).
[38] S. Ayik, B. Yilmaz, O. Yilmaz, and A. S. Umar, Phys. Rev. C **97**, 054618 (2018).
[39] V. Yu. Denisov, and I. Yu. Sedykh, Chin. Phys. C **45**, 084002 (2021).
[40] X.-X. Sun and L. Guo, Phys. Rev. C **107**, 064609 (2023).
[41] W. J. Swiatecki, K. Siwek-Wilczynska, and J. Wilczynski, Int. J. Mod. Phys. E **13**, 261 (2004).
[42] T. I. Nevzorova and G. I. Kosenko, Phys. At. Nucl. **71**, 1373 (2008).
[43] Y. Abe, C. Shen, D. Boilley, B. G. Giraud, and G. Kosenko, Nucl. Phys. A **834**, 349c (2010).
[44] A. S. Umar, V. E. Oberacker, and C. Simenel, Phys. Rev. C **94**, 024605 (2016).
[45] K. Sekizawa and K. Yabana, Phys. Rev. C **93**, 054616 (2016).
[46] K. Godbey, A. S. Umar, and C. Simenel, Phys. Rev. C **100**, 024610 (2019).
[47] P. McGlynn and C. Simenel, Phys. Rev. C **107**, 054614 (2023).

[48] S. Amano, Y. Aritomo, and M. Ohta, Phys. Rev. C **106**, 024610 (2022).
[49] V. I. Zagrebaev and W. Greiner, Nucl. Phys. A **944**, 257 (2015).
[50] K. P. Santhosh and V. Safoora, Phys. Rev. C **96**, 034610 (2017).
[51] P. S. DamodaraGupta, N. Sowmya, H. C. Manjunatha, L. Seenappa, and T. Ganesh, Phys. Rev. C **106**, 064603 (2022).
[52] D. Glas and U. Mosel, Nucl. Phys. A **237**, 429 (1975).
[53] P. Frobrich and R. Lipperheide, *Theory of Nuclear Reactions* (Clarendon Press, Oxford, 1996).
[54] D. H. E. Gross and H. Kalinowski, Phys. Rep. **45**, 175 (1978).
[55] P. Fröbrich, Phys. Rep. **116**, 337 (1984).
[56] S. Bjørnholm and W. J. Swiatecki, Nucl. Phys. A **391**, 471 (1982).
[57] J. P. Blocki, H. Feldmeier, and W. J. Swiatecki, Nucl. Phys. A **459**, 145 (1986).
[58] V. V. Volkov, Izv. Akad. Nauk SSSR, Ser. Fiz. **50**, 1879 (1986) [Bull. Acad. Sci. USSR, Phys. Ser. **50**, 6 (1986)].
[59] S. Soheyli and M. V. Khanlari, Phys. Rev. C **94**, 034615 (2016).
[60] P. Eudes, Z. Basrak, F. Sébille, V. delaMota, and G. Royer, Phys. Rev. C **90**, 034609 (2014).
[61] D. Dell'Aquila *et al.*, Phys. Lett. B **837**, 137642 (2023).
[62] D. Dell'Aquila *et al.*, J. Phys. G **50**, 015101 (2023).
[63] H. Eslamizadeh and H. Falinejad, Phys. Rev. C **105**, 044604 (2022).
[64] V. Yu. Denisov and W. Norenberg, Eur. Phys. J. A **15**, 375 (2002).
[65] C. Riedel, G. Wolschin, and W. Norenberg, Z. Phys. A **290**, 47 (1979).
[66] C. Simenel and A. S. Umar, Prog. Part. Nucl. Phys. **103**, 19 (2018).
[67] S. Ayik and K. Sekizawa, Phys. Rev. C **102**, 064619 (2020).
[68] N. Bohr and J. A. Wheeler, Phys. Rev. **56**, 426 (1939).
[69] C. Simenel, K. Godbey, and A. S. Umar, Phys. Rev. Lett. **124**, 212504 (2020).
[70] A. Wakhle, C. Simenel, D. J. Hinde, M. Dasgupta, M. Evers, D. H. Luong, R. duRietz, and E. Williams, Phys. Rev. Lett. **113**, 182502 (2014).
[71] M. Mirea, R. Budaca, and A. Sandulescu, Ann. Phys. (NY) **380**, 154 (2017).
[72] Z. Ahmed, Phys. Lett. A **157**, 1 (1991).
[73] P. M. Morse, Phys. Rev. **34**, 57 (1929).
[74] V. Yu. Denisov, Phys. Rev. C **107**, 054618 (2023).
[75] C. Kemble, Phys. Rev. **48**, 549 (1935).
[76] D. L. Hill and J. A. Wheeler, Phys. Rev. **89**, 1102 (1953).
[77] W. U. Schroder and J. R. Huizenga, Annu. Rev. Nucl. Sci. **27**, 465 (1977).
[78] V. V. Volkov, Phys. Rep. **44**, 93 (1978).
[79] M. Brack *et al.*, Rev. Mod. Phys. **44**, 320 (1972).
[80] V. M. Strutinsky, Yad. Fiz. **3**, 604 (1966) [Sov. J. Nucl. Phys. **3**, 449 (1966)].
[81] V. M. Strutinsky, Nucl. Phys. A **95**, 420 (1967).
[82] V. M. Strutinsky, Nucl. Phys. A **122**, 1 (1968).
[83] G. D. Adeev and P. A. Cherdantsev, Phys. Lett. B **39**, 485 (1972).
[84] M. Brack and Ph. Quentin, Phys. Scr. **10**, 163 (1974).
[85] M. Diebel, K. Albrecht, and R. W. Hasse, Nucl. Phys. A **355**, 66 (1981).
[86] Z. Lojewski, V. V. Pashkevich, and S. Cwiok, Nucl. Phys. A **436**, 499 (1985).
[87] J. A. Sheikh, W. Nazarewicz, and J. C. Pei, Phys. Rev. C **80**, 011302(R) (2009).
[88] J. C. Pei *et al.*, Nucl. Phys. A **834**, 381c (2010).
[89] V. Yu. Denisov and I. Yu. Sedykh, Eur. Phys. J. A **54**, 231 (2018).
[90] V. Yu. Denisov and I. Yu. Sedykh, Phys. Rev. C **98**, 024601 (2018).
[91] O. I. Davydovska, V. Yu. Denisov, and I. Yu. Sedykh, Phys. Rev. C **105**, 014620 (2022).
[92] W. Dilg *et al.*, Nucl. Phys. A **217**, 269 (1973).
[93] R. Capote *et al.*, Nucl. Data Sheets **110**, 3107 (2009).
[94] A. V. Ignatyuk, G. N. Smirenkin, and A. S. Tishin, Yad. Fiz. **21**, 485 (1975) [Sov. J. Nucl. Phys. **21**, 255 (1975)].
[95] A. Mengoni and Y. Nakajima, J. Nucl. Sci. Technol. **31**, 151 (1994).
[96] M. Brack, C. Guet, and H.-B. Hakannson, Phys. Rep. **123**, 275 (1985).
[97] C. Guet, E. Strumberger, and M. Brack, Phys. Lett. B **205**, 427 (1988).
[98] P. Moller *et al.*, At. Data Nucl. Data Tables **109-110**, 1 (2016).
[99] P. Jachimowicz, M. Kowal, and J. Skalski, At. Data Nucl. Data Tables **138**, 101393 (2021).
[100] A. J. Sierk, Phys. Rev. C **33**, 2039 (1986).
[101] P. Möller, A.J. Sierk, T. Ichikawa, A. Iwamoto, and M. Mumpower, Phys. Rev. C **91**, 024310 (2015).
[102] P. Möller, Nucl. Phys. A **192**, 529 (1972).
[103] H. Abusara, A. V. Afanasjev, and P. Ring, Phys. Rev. C **85**, 024314 (2012).
[104] D. A. Varshalovich, A. N. Moskalev, and V. K. Khersonsky, *Quantum Theory of Angular Momentum: Irreducible Tensors, Spherical Harmonics, Vector Coupling Coefficients, 3nj Symbols* (World Scientific, Singapore, 1988).
[105] V. Yu. Denisov and N. A. Pilipenko, Phys. Rev. C **76**, 014602 (2007).
[106] V. Yu. Denisov, Eur. Phys. J. A **58**, 91 (2022).
[107] A. Bohr and B. Mottelson, *Nuclear Structure* (W. A. Benjamin, New York, 1974), Vol. 2.
[108] V. Yu. Denisov, Yad. Fiz. **49**, 644 (1989) [Sov. J. Nucl. Phys. **49**, 399 (1989)].
[109] V. Yu. Denisov and O. I. Davidovskaya, Yad. Fiz. **59**, 981 (1996) [Phys. At. Nucl. **59**, 938 (1996)].
[110] B. V. Derjaguin, Kolloid-Z. **69**, 155 (1934).
[111] J. Blocki *et al.*, Ann. Phys. (NY) **105**, 427 (1977).
[112] V. Yu. Denisov, Phys. Rev. C **91**, 024603 (2015).
[113] I. Dutt and R. K. Puri, Phys. Rev. C **81**, 064609 (2010).
[114] V. Yu. Denisov, Phys. Lett. B **526**, 315 (2002).
[115] V. Yu. Denisov, T. O. Margitych, and I. Yu. Sedykh, Nucl. Phys. A **958**, 101 (2017).
[116] V. Yu. Denisov and I. Yu. Sedykh, Nucl. Phys. A **963**, 15 (2017).
[117] V. Yu. Denisov, Phys. Rev. C **89**, 044604 (2014).
[118] J. Maruhn and W. Greiner, Z. Phys. **251**, 431 (1972).
[119] M. Mirea, A. Sandulescu, and D. S. Delion, Nucl. Phys. A **870-871**, 23 (2011).
[120] F. G. Kondev *et al.*, Chin. Phys. C **45**, 030001 (2021).
[121] C. Y. Wong, Nucl. Data A **4**, 271 (1968).
[122] V. Yu. Denisov, Eur. Phys. J. A **58**, 188 (2022).
[123] E.F. Aguilera, J.J. Kolata, P.A. DeYoung, and J.J. Vega, Phys. Rev. C **33**, 1961 (1986).

[124] Y. Nagashima *et al.*, Phys. Rev. C **33**, 176 (1986).
[125] M. F. Vineyard *et al.*, Phys. Rev. C **41**, 1005 (1990).
[126] S. B. DiCenzo, J. F. Petersen, and R. R. Betts, Phys. Rev. C **23**, 2561 (1981).
[127] R. J. Meijer *et al.*, Phys. Rev. C **44**, 2625 (1991).
[128] A. Oberstedt *et al.*, Nucl. Phys. A **548**, 525 (1992).
[129] G. Montagnoli *et al.*, Phys. Rev. C **90**, 044608 (2014).
[130] A. Sandulescu, D. N. Poenaru, and W. Greiner, Fiz. Elem. Chastits At. Yadra **11**, 1334 (1980) [Sov. J. Part. Nucl. **11**, 528 (1980)].
[131] G. Royer, R. K. Gupta, and V. Yu. Denisov, Nucl. Phys. A **632**, 275 (1998).
[132] H. C. Britt *et al.*, Phys. Rev. C **13**, 1483 (1976).
[133] H. Oeschler, H. Freiesleben, K. D. Hildenbrand, P. Engelstein, J. P. Coffin, B. Heusch, and P. Wagner, Phys. Rev. C **22**, 546 (1980).
[134] L. M. Robledo and J. L. Egido, AIP Conf. Proc. **798**, 103 (2005).
[135] R. Bock *et al.*, Nucl. Phys. A **388**, 334 (1982).
[136] H.-G. Clerc *et al.*, Nucl. Phys. A **419**, 571 (1984).
[137] V. Yu. Denisov, Phys. At. Nucl. **68**, 1133 (2005).
[138] M. Warda, A. Zdeb, and L. M. Robledo, Phys. Rev. C **98**, 041602(R) (2018).
[139] Z. Matheson, S. A. Giuliani, W. Nazarewicz, J. Sadhukhan, and N. Schunck, Phys. Rev. C **99**, 041304(R) (2019).